Supplementary Information

Anion control of tautomeric equilibria: FeH vs. NH influenced by NH•••F hydrogen bonding

Geoffrey M. Chambers, Samantha I. Johnson, Simone Raugei and R. Morris Bullock*

Center for Molecular Electrocatalysis, Pacific Northwest National Laboratory,
Richland, Washington 99352, United States

Experimental Section

Syntheses and Materials. All preparations and manipulations were performed under an argon atmosphere. Solvents were dried using activated alumina columns and stored under Ar. $Fe(COT)(CO)_3$ was purchased from Strem Chemical Company and used as received. The diphosphines $P^{Et}N^{Me}P^{Et}$,[1] $P^{Et}N^{Ph}P^{Et}$,[2] $(PAr^F{}_2)_2CH_2$,[3] depp (1,3-bis(diethylphosphino)propane),[4] $CpCr(CO)_3H$,[5] $CpMo(CO)_3$,[6] $Cp^*Cr(CO)_3H$,[7] $[Cp_2Fe]^+[BAr^F{}_4]^-$,[8] and $[(Et_2O)_2H]^+[B(C_6F_5)_4]^-$[9] were prepared according to published procedures. The electrolyte $[Bu_4N]^+[B(C_6F_5)_4]^-$ was prepared and purified using established procedures.[10] The amine *p*-anisidine was purified by sublimation. (2,2,6,6-Tetramethylpiperidin-1-yl)oxyl (TEMPO) was purified by sublimation. 2,6-di-*tert*-butylpyridine and 2,6-lutidine were dried over KOH for 48h, then distilled under reduced pressure.

Electrochemistry. Cyclic voltammograms were recorded under Ar in a glovebox in 0.1 M $[Bu_4N][B(C_6F_5)_4]$ electrolyte solutions in PhF, or 0.1 M $[Bu_4N]PF_6$ electrolyte solutions in CH_2Cl_2 at ambient temperature, 20-22 °C. Cyclic voltammetry experiments, using a standard three-electrode configuration, were conducted using a CHI 660C potentiostat interfaced with a computer using CHI 700D software. Cyclic voltammetric scans were recorded using a glassy carbon working electrode with 1 mm disc diameter, a silver wire pseudoreference electrode, and a platinum wire counter electrode.. All potentials were referenced to the $[Cp_2Fe]^{0/+}$ couple using the $[Cp_2Co]^{+/0}$ couple (-1.33 V vs $[Cp_2Fe]^{0/+}$) as a secondary standard. The salts $[Cp_2Co]^+[B(C_6F_5)_4{}^-$ and $[Cp_2Co]^+PF_6^-$ were used as a secondary internal standard for experiments conducted in PhF and CH_2Cl_2, respectively.

Single Crystal X-ray Diffraction. Suitable single crystals immersed in Paratone oil were identified using a microscope, mounted on a nylon loop, and placed under a cold stream of nitrogen. Unless otherwise noted, crystallographic data were recorded at 100 K. Crystallographic data were collected using a Bruker KAPPA APEX II CCD diffractometer equipped with a Mo Kα source (λ = 0.71073 Å). Space groups were determined on the basis of systemic absences and intensity statistics. Structure solutions were determined using intrinsic phasing and refined by full-matrix least squares on F^2. Data collection and cell refinement were performed using Bruker APEX3 software. Data reduction and absorption corrections were performed using SAINT and SADABS.[11, 12] Structure solution and refinement were accomplished using the SHELX-97 and OLEX2[13] software packages.

Spectroscopy. NMR spectra were recorded on a Varian Inova spectrometers (500 MHz for ^1H) at 22°C. ^1H chemical shifts were referenced internally using the residual proton resonance of the deuterated solvent. ^{31}P NMR spectra were referenced to an external 85% H_3PO_4 standard. ^{19}F NMR spectra were referenced to external fluorobenzene at −135.15 ppm. EPR spectra were recorded using a Bruker E580 spectrometer equipped with a SHQE resonator and a continuous flow cryostat. Spectra were recorded at 125K suspended in a frozen toluene glass (1-5 mM) contained in 4 mm OD quartz tubes. Microwave power was typically 2 milliwatts, and the frequency was 9.32 GHz. IR spectra were recorded on a Thermo Scientific Nicolet iS10 FTIR spectrometer using CaF_2 solution cells or a KBr pellet.

$Fe(P^{Et}N^{Me}P^{Et})(CO)_3$ (Fe^0). A 3 mL solution of $Fe(COT)(CO)_3$ (17.0 mg, 0.069 mmol) in toluene was treated with $P^{Et}N^{Me}P^{Et}$ (20.0 mg, 0.085 mmol) in 3 mL of toluene. The deep red mixture was heated to 110 °C overnight. The solvent was removed from the resultant pale yellow solution by evaporation under reduced pressure. The product was purified by silica gel chromatography under argon. Unreacted material and side products elute with 100% *n*-pentane, and compound **1** elutes with 100% CH_2Cl_2 as a dark yellow band. Evaporation of the solvent gave $Fe(P^{Et}N^{Me}P^{Et})(CO)_3$ as a pale yellow crystalline solid that was recrystallized by evaporation from Et_2O solution. Yield: 20.3 mg (78 %). ^{1}H NMR (CD_2Cl_2): δ 2.55 (s, 4H, PC*H*$_2$N), 2.36 (s, 3H N-C*H*$_3$), 1.72 (m, 8H, PC*H*$_2$CH$_3$), 1.10 (m, 12H, PCH$_2$C*H*$_3$). ^{31}P{^{1}H} NMR (CD_2Cl_2): δ 39.3 (s). IR (CH_2Cl_2): $\tilde{\nu}_{CO}$ = 1976 (s), 1900 (s), 1873 (s) cm^{-1}. Anal. Calcd (found) for $C_{14}H_{27}FeNO_3P_2$: C, 44.82 (44.89); H, 7.25 (7.33); N, 3.73 (3.75). Single crystals for x-ray diffraction were grown by evaporation of *n*-pentane solutions.

$Fe(P^{Et}N^{Ph}P^{Et})(CO)_3$. This complex was prepared in a similar manner to $Fe(P^{Et}N^{Me}P^{Et})(CO)_3$ (**Fe^0**), and was isolated as pale yellow crystals. Yield: 63 %. ^{1}H NMR (CD_2Cl_2): δ 7.30 (t, 2H, *J* = 7.9 Hz, Ar-*H*), 6.96 (m, 3H, Ar-*H*), 3.41 (s, 4H, PC*H*$_2$N), 1.80 (m, 8H, PC*H*$_2$CH$_3$), 1.14 (m, 12H, PCH$_2$C*H*$_3$). ^{31}P{^{1}H} NMR (CD_2Cl_2): δ 37.5. IR (CH_2Cl_2): $\tilde{\nu}_{CO}$ = 1978 (s), 1903 (s), 1877 (s) cm^{-1}. Anal. Calcd (found) for $C_{19}H_{29}FeNO_3P_2$: C, 52.19 (52.18); H, 6.69 (6.72); N, 3.20 (3.22).

$[Fe(P^{Et}N^{Me}P^{Et})(CO)_3]^+BAr^F{}_4^-$ ($[Fe^I]^+BAr^F{}_4^-$). A solution of **Fe^0** (13.4 mg, 35.7 μmol) in Et_2O (3 mL) was treated with $[Cp_2Fe][BAr^F{}_4]$ (37.2 mg, 35.5 μmol) in Et_2O (2 mL). The pale yellow solution instantly became dark green. The solvent was removed under reduced pressure, and the resultant residue was washed several times with pentane until the washings were colorless. The residue was dissolved in Et_2O, and the product was crystallized by slow addition of pentane and isolated as a dark green microcrystalline powder. Yield: 39.8 mg (91%). IR (CH_2Cl_2): $\tilde{\nu}_{CO}$ = 2069 (s), 2007 (m), 1999 (m) cm^{-1}. Anal. Calcd (found) for $C_{46}H_{39}BF_{24}FeNO_3P_2$: C, 44.61 (44.55); H, 3.17 (3.21); N, 1.13 (1.10). Single crystals were grown by vapor diffusion of *n*-pentane into a concentrated Et_2O solution.

$[Fe(P^{Et}N^{Ph}P^{Et})(CO)_3]^+BAr^F{}_4^-$. This complex was prepared in a similar manner to $[Fe^I]^+[BAr^F{}_4]^-$. Yield: 93%. IR (CH_2Cl_2): $\tilde{\nu}_{CO}$ = 2070 (s), 2008 (m), 1999 (m) cm^{-1}.

$[Fe(P^{Et}N^{Ph}P^{Et})(CO)_3H]^+[B(C_6F_5)_4]^-$. A solution of $[(Et_2O)_2H]^+[B(C_6F_5)_4]^-$ (29.0 mg, 28.6 μmol) in Et_2O (3 mL) was added to a 3 mL solution of $Fe(P^{Et}N^{Ph}P^{Et})(CO)_3$ (11.0 mg, 29.3 μmol) in Et_2O. The mixture was filtered through Celite, and the solvent was removed under reduced pressure, giving a pale yellow oil. The residue was dissolved in 1 mL of Et_2O, the product was precipitated by slow addition of pentane (5 mL). Evaporation of the solvent gave $[Fe(P^{Et}N^{Ph}P^{Et})(CO)_3H]^+[B(C_6F_5)_4]^-$ as a white amorphous solid. Yield: 28.1 mg (79%) ^{1}H NMR (CD_2Cl_2): δ 7.39 (t, 2H, *J* = 8.0 Hz, Ar-*H*), 7.17 (t, 1H, *J* = 7.2 Hz, Ar-*H*), 7.00 (d, 2H, *J* = 8.5 Hz, Ar-*H*), 3.76 (2H, m, PC*H*$_2$N), 3.52 (2H, d, $^2J_{HH}$ = 14 Hz, PC*H*$_2$N), 2.05 (m, 8H, PC*H*$_2$CH$_3$), 1.27 (m, 12H, PCH$_2$C*H*$_3$), −9.12 (t, 1H, J_{PH} = 45.5 Hz, M-*H*). ^{31}P{^{1}H} NMR (CD_2Cl_2): δ 33.9 (s). IR (CH_2Cl_2): $\tilde{\nu}_{CO}$ = 2090 (s), 2035 (br). Anal. Calcd (found) for $C_{40}H_{30}BF_{20}FeNO_3P_2$: C,

46.50 (46.17); H, 2.92 (2.76); N, 1.36 (1.34). Single crystals for X-ray diffraction were grown by vapor diffusion of *n*-pentane into a concentrated Et_2O solution.

[Fe(P^{Et}N^{Me}P^{Et})(CO)$_3$H]$^+$BAr$^F_4$$^-$ ([FeH]BAr$^F_4$**).** The complex [**FeH**]BAr$^F_4$ was prepared in a similar manner as compound [Fe(P^{Et}N^{Ph}P^{Et})(CO)$_3$H]$^+$BAr$^F_4$$^-$. Yield: 85%. ^{1}H NMR (CD_2Cl_2): δ 3.02 (2H, m, (PC*H*$_2$)$_2$NMe), 2.79 (2H, d, $^2J_{HH}$ = 14 Hz, (PC*H*$_2$)$_2$NMe), 2.51 (3H, s, (PC*H*$_2$)$_2$NC*H*$_3$), 1.97 (8H, m, PC*H*$_2$CH$_3$), 1.24 (12H, m, PCH$_2$C*H*$_3$), −9.27 (t, 1H, J_{PH} = 45.1 Hz). ^{31}P{^{1}H} NMR (CD_2Cl_2): δ 33.2. IR (CH_2Cl_2): $\tilde{\nu}_{CO}$ = 2089 cm^{-1} (s), 2033 (s) cm^{-1}. Anal. Calcd (found) for $C_{38}H_{28}BF_{20}FeNO_3P_2$: C, 43.25 (43.70); H 2.67 (3.03); N 1.33 (1.47).

[Fe(P^{Et}N^{Me}P^{Et})(CO)$_3$H]$^+$BF$_4$ ([FeNH]BF$_4$**).** A solution of **Fe^0** (22.4 mg, 59.7 μmol) in MeCN (3 mL) was treated with a solution of HBF$_4$·Et$_2$O (9.2 mg, 56.7 μmol, 0.95 equiv.) in MeCN (3 mL). The yellow solution immediately lightened, becoming nearly colorless. The product was crystallized by the addition of Et_2O (5 mL). Yield: 23.4 mg (89%). Single crystals for X-ray diffraction were grown by vapor diffusion of Et_2O into concentration Et_2O solution. ^{1}H NMR (CD_2Cl_2): δ 3.30 (2H, m, (PC*H*$_2$)$_2$NMe), 2.90 (2H, m, (PC*H*$_2$)$_2$NMe), 2.80 (3H, s, (PC*H*$_2$)$_2$NC*H*$_3$), 1.95 (8H, m (br), PC*H*$_2$CH$_3$). 1.24 (12H, m (br), PCH$_2$C*H*$_3$). ^{31}P{^{1}H} NMR (CD_2Cl_2): δ 39.0 (br). IR (KBr): $\tilde{\nu}_{CO}$ = 1993 cm^{-1} (s), 1934 (s) cm^{-1}, 1890 (s) cm^{-1}. $\tilde{\nu}_{NH}$ = 3142 (br)

[Fe(depp)(CO)$_3$H]$^+$BF$_4$$^-$. [Fe(depp)(CO)$_3$H]$^+BF_4$$^-$ was prepared in a similar manner as [Fe(P^{Et}N^{Ph}P^{Et})(CO)$_3$H]BAr$^F_4$ using HBF$_4$·Et$_2$O as the acid. Yield: 94%. ^{1}H NMR (CD_2Cl_2): δ 1.92 (14H, m, (PC*H*$_2$)$_2$C*H*$_2$ and PC*H*$_2$CH$_3$), 1.23 (12H, m, PCH$_2$C*H*$_3$), −9.03 (t, 1H, J_{PH} = 44.76 Hz). ^{31}P{^{1}H} NMR (CD_2Cl_2): δ 34.31. IR (CH_2Cl_2): $\tilde{\nu}_{CO}$ = 2089 cm^{-1} (s), 2033 (s) cm^{-1}.

[Fe(P^{Et}N^{Me}P^{Et})(CO)$_3$H]$^+$OTf$^-$ ([FeNH]OTf**).** The complex **[FeNH]**OTf was prepared in a similar manner as **[FeNH]**BF$_4$ Yield: 92%.

[Fe(P^{Et}N^{Me}HP^{Et})(CO)$_3$H][OTf]$_2$ ([FeHNH][OTf]$_2$). A solution of **Fe^0** (28.7 mg, 76.5 μmol) in MeCN (3 mL) was treated with HOTf (24.5 mg, 163.3 μmol) in MeCN (2 mL). The pale yellow solution became colorless after the addition. The solvent was evaporated under reduced pressure to a volume of ~ 0.5 mL, and the doubly protonated salt was precipitated with Et_2O. The product was washed several times with Et_2O and dried under vacuum. Yield: 38.7 mg (83%). ^{1}H NMR (CD_3CN) (Mixture of *cis* and *trans* isomers): δ 9.40 (s, br, 1H, N*H*Me), 8.89 (s, br, 1H, N*H*Me), 4.04 (d, 2H, *J* = 14 Hz, 2H, PC*H*$_2$NMe), 3.98 (d, 2H, *J* = 14 Hz, 2H, PC*H*$_2$NMe), 3.54 (dd, 2H, *J* = 15, 10 Hz, PC*H*$_2$NMe), 3.45 (dd, 2H, *J* = 15, 10 Hz, PC*H*$_2$NMe), 3.24 (s, br, 6H NC*H*$_3$), 2.25 (m, 16H, PC*H*$_2$CH$_3$), 1.23 (m, br, 24H, PCH$_3$C*H*$_3$). −9.62 (s, br, 1H, Fe*H*), −9.72 (s, br, 1H, Fe*H*). ^{31}P{^{1}H} NMR (CD_3CN): δ 45.8 (s), 45.6 (s). IR (KBr): $\tilde{\nu}_{NH}$ = 3142 (br). $\tilde{\nu}_{CO}$ = 2103 (m), 2042 (s, br) cm^{-1}. Anal. Calcd (found) for $C_{16}H_{29}F_6FeNO_9P_2S_2$: C, 28.46 (28.46); H, 4.33 (4.36); N, 2.07 (2.20). Single crystals were grown by vapor diffusion of Et_2O into a concentrated MeCN solution.

NMR Spectra

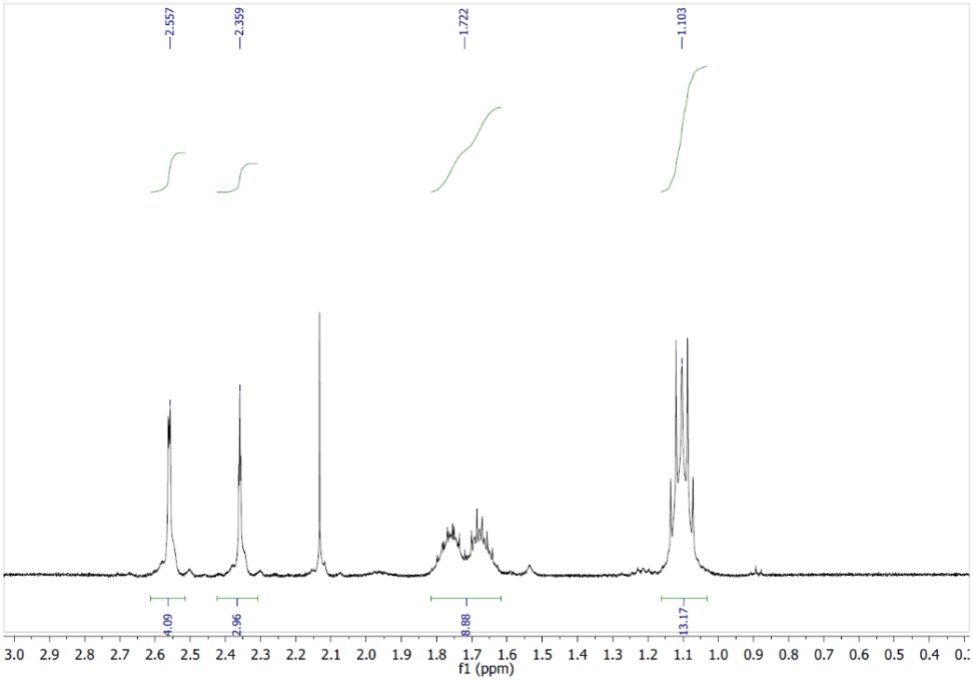

Figure S1. ^{1}H NMR spectrum of Fe($P^{Et}N^{Me}P^{Et}$)$(CO)_3$ (**Fe^{0}**) in CD_2Cl_2.

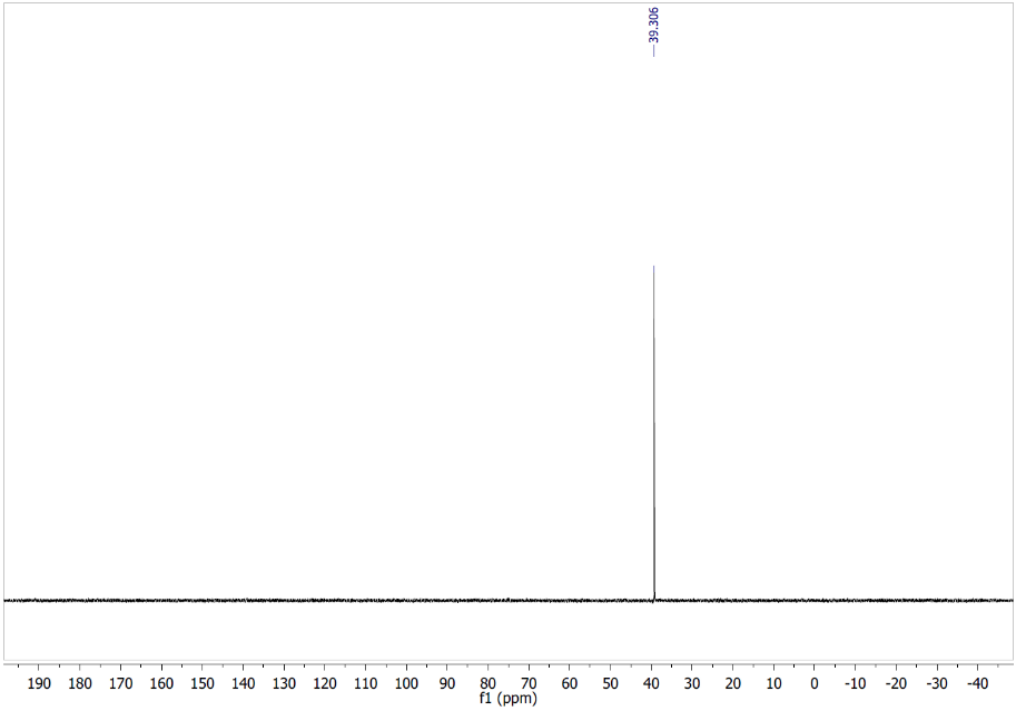

Figure S2. ^{31}P{^{1}H} NMR spectrum of Fe($P^{Et}N^{Me}P^{Et}$)$(CO)_3$ (**Fe^{0}**) in CD_2Cl_2.

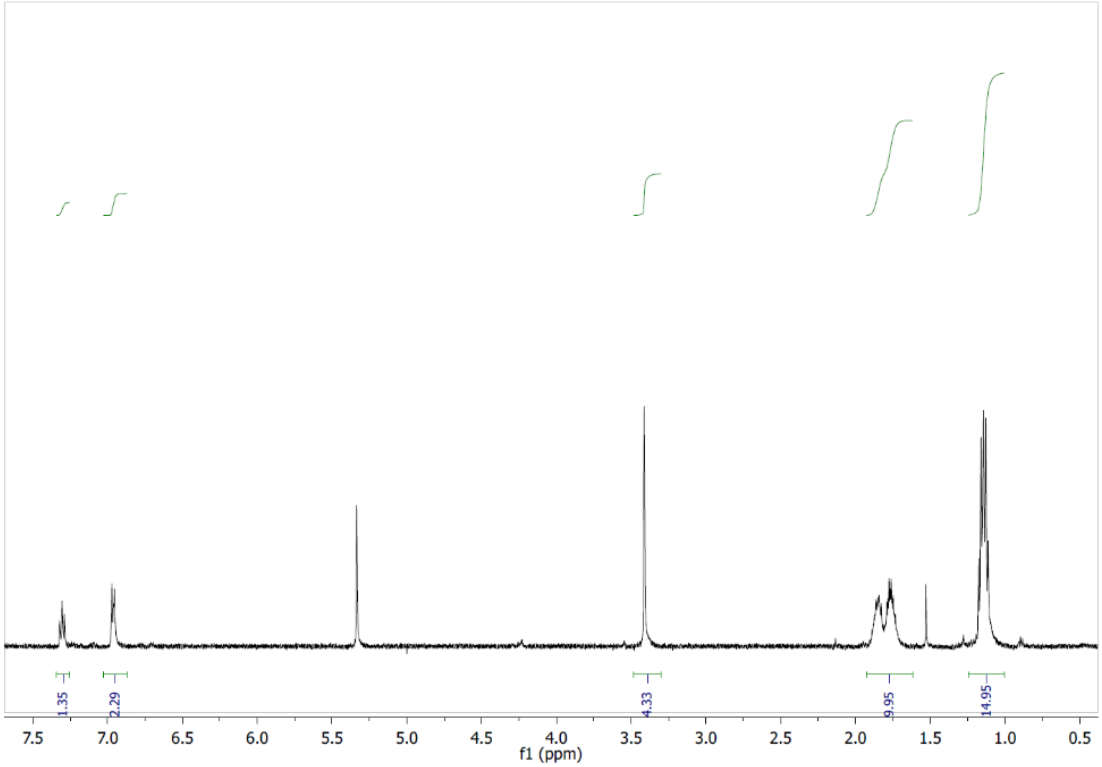

Figure S3. ^{1}H NMR spectrum of Fe($P^{Et}N^{Ph}P^{Et}$)$(CO)_3$ in CD_2Cl_2.

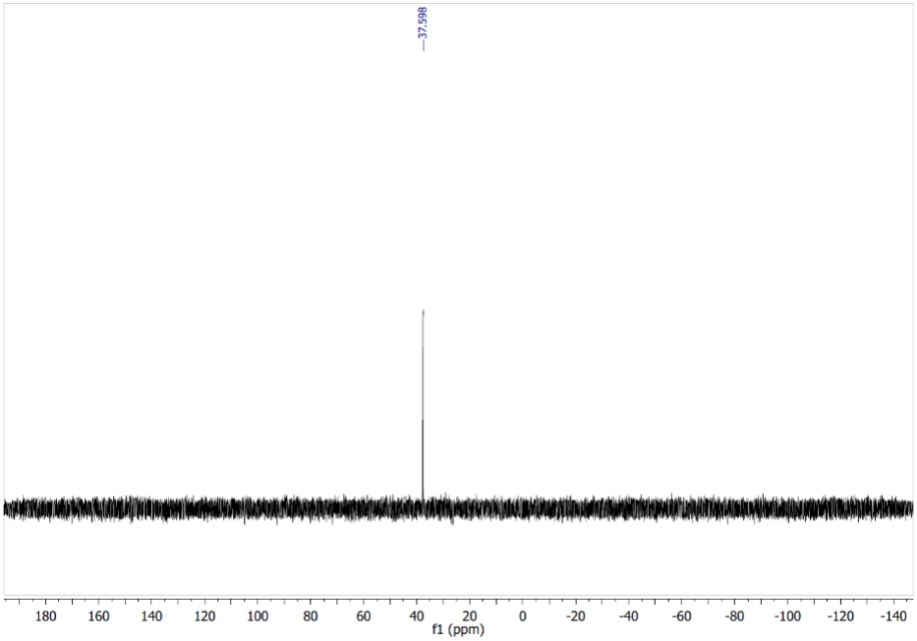

Figure S4. ^{31}P{^{1}H} NMR spectrum of Fe($P^{Et}N^{Ph}P^{Et}$)$(CO)_3$ in CD_2Cl_2.

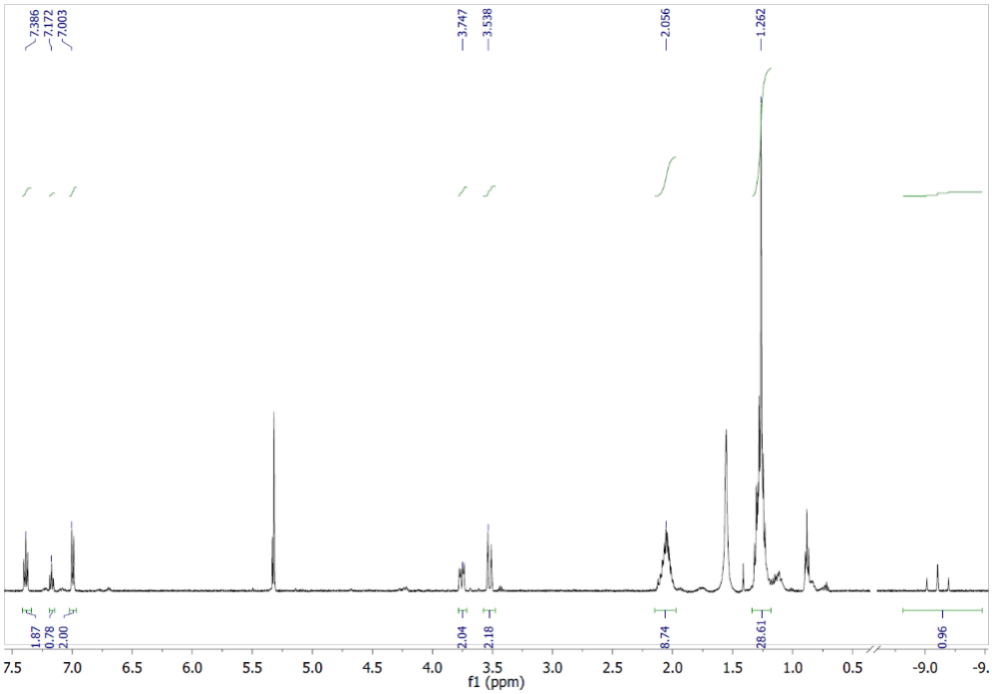

Figure S5. ^{1}H NMR spectrum of $[Fe(P^{Et}N^{Ph}P^{Et})(CO)_3H][B(C_6F_5)_4]$ in CD_2Cl_2.

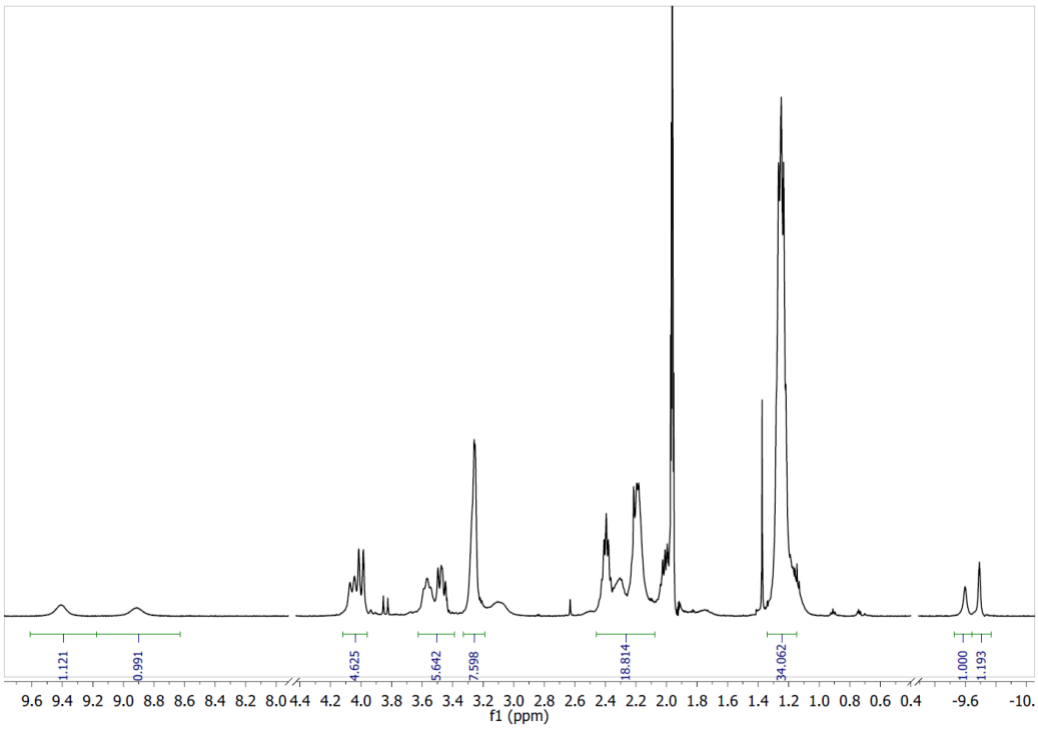

Figure S6. ^{1}H{^{31}P} NMR spectrum of [**FeHNH**][OTf]$_2$ in CD_3CN at 23 °C.

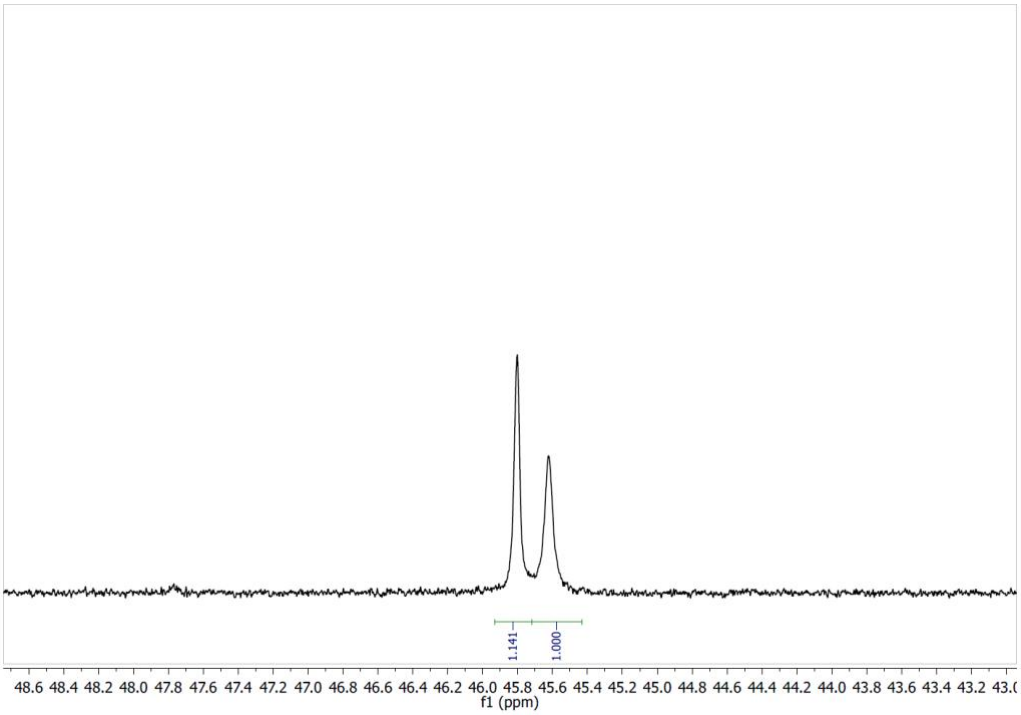

Figure S7. $^{31}P\{^{1}H\}$ NMR spectrum of [**FeHNH**][OTf]$_2$ in CD_3CN at 23 °C.

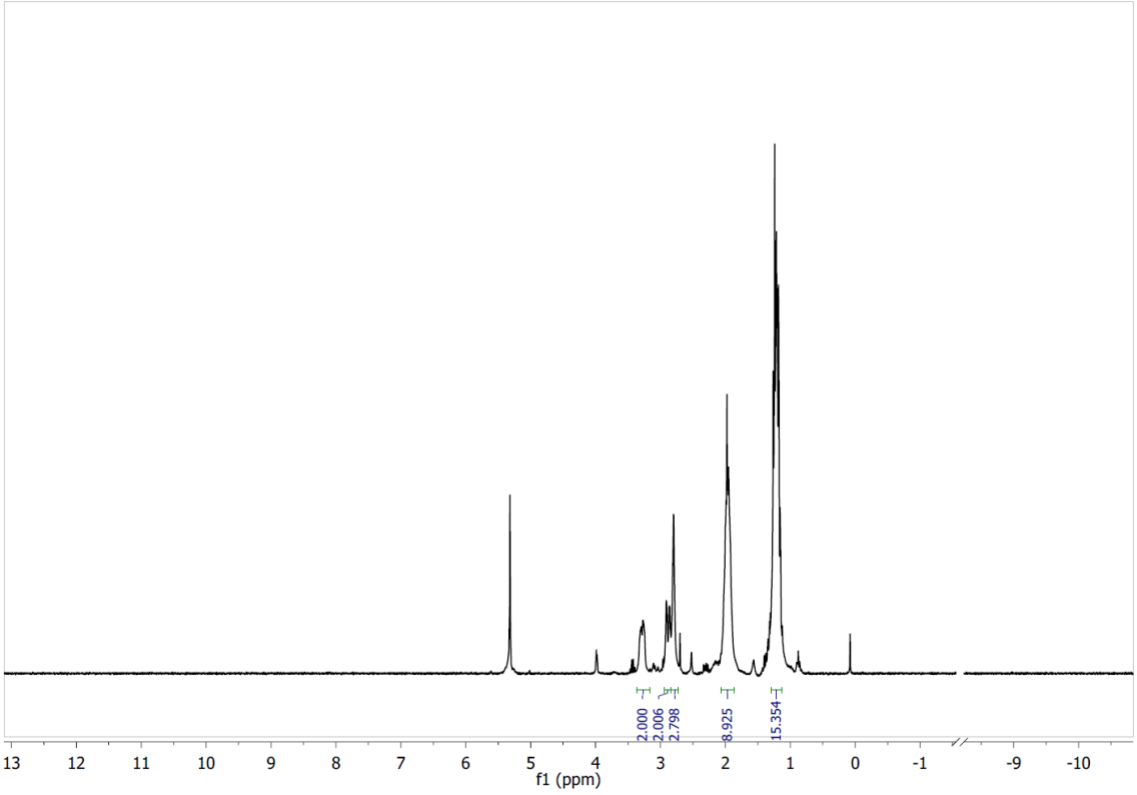

Figure S8. ^{1}H NMR spectrum in CD_2Cl_2 of [**FeNH**]BF_4 crystals mechanically isolated from crystallization crop.

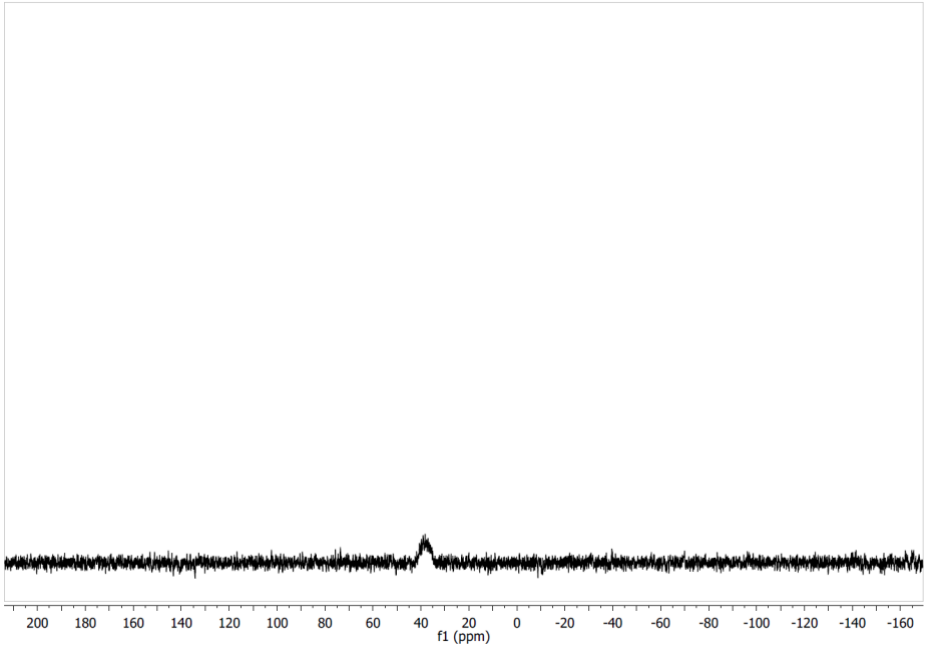

Figure S9. $^{31}P\{^{1}H\}$ NMR spectrum in CD_2Cl_2 of [**FeNH**]BF_4 crystals manually isolated from the crystallization crop.

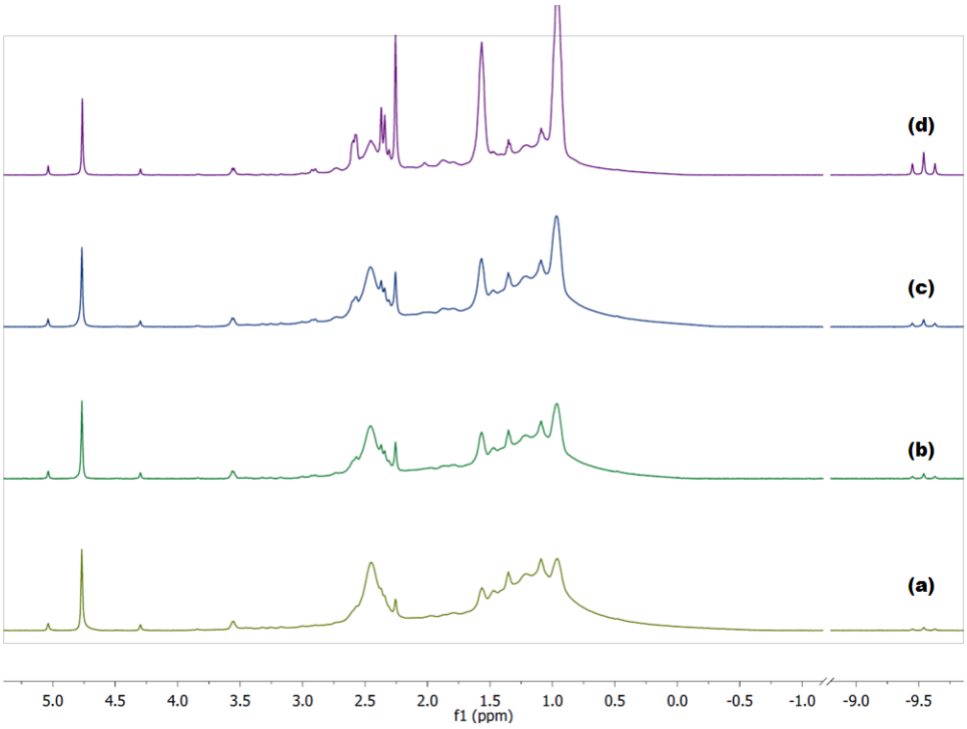

Figure S10. Stacked ^{1}H NMR spectra of [**Fe**]$^{+}$[$B(C_6F_5)_4$]$^{-}$ in C_6D_5Br under H_2 over time. (a) 1h. (b) 3h. (c) 6h. (d) 24h.

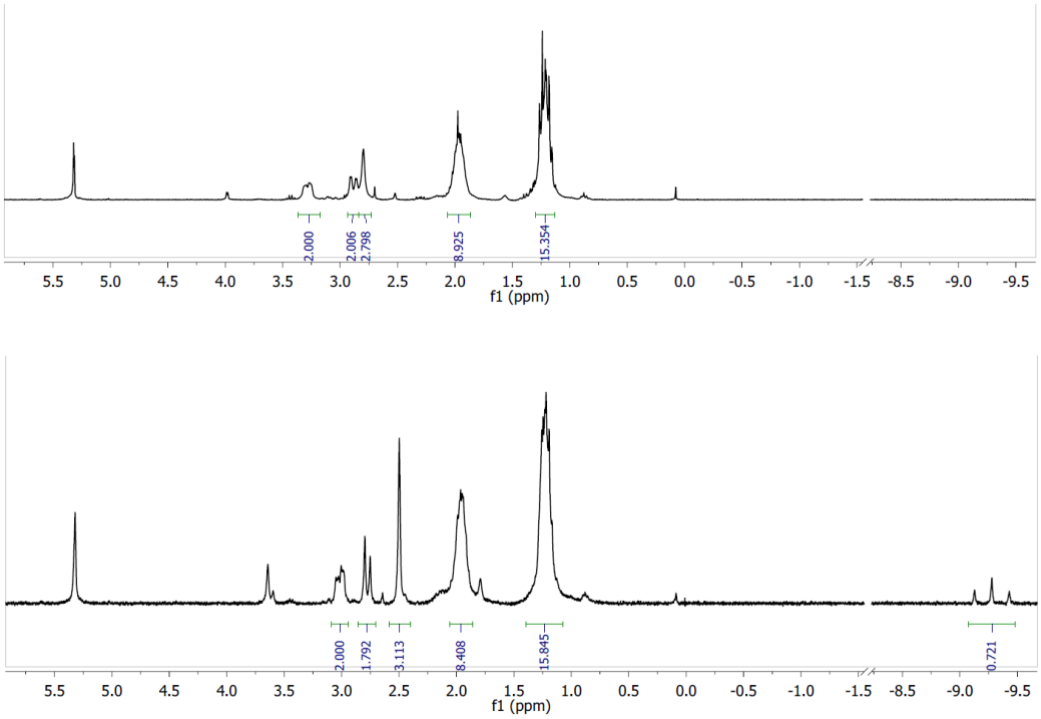

Figure S11. ^{1}H NMR Spectra. (top) [**FeNH**]BF_4 in CD_2Cl_2.
(bottom) [**FeNH**]BF_4 with excess K[B(C_6F_5)$_4$] in CD_2Cl_2 and added THF-*d*$_8$.

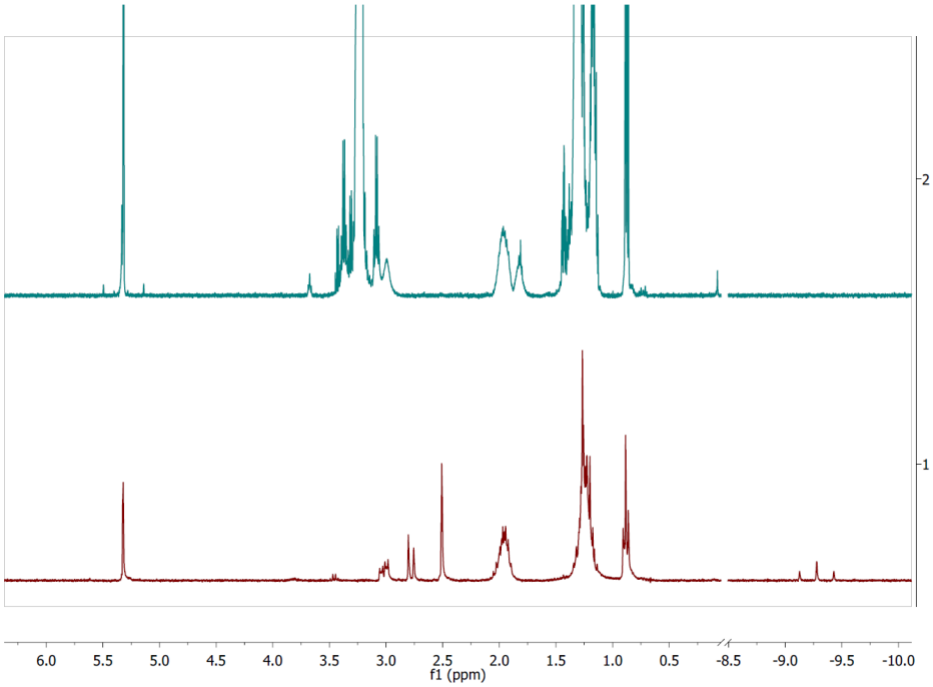

Figure S12. ^{1}H NMR Spectra. (bottom) [**FeH**][B(C_6F_5)$_4$] in CD_2Cl_2. (top) [**FeH**][B(C_6F_5)$_4$] with excess [Et_4N][BF_4] in CD_2Cl_2.

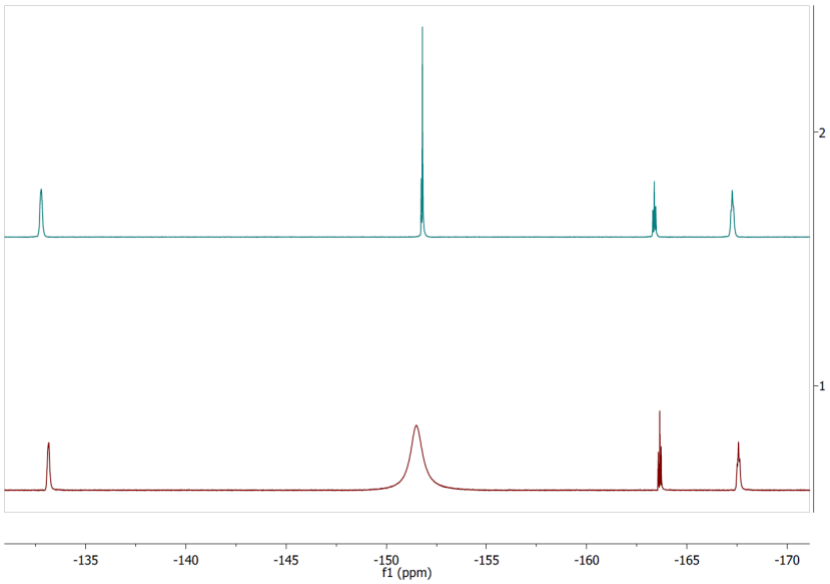

Figure S13. ^{19}F NMR Spectra. (top) $[Et_4N][BF_4]$ and $[Bu_4N][B(C_6F_5)_4]$ in CH_2Cl_2. (bottom) [**FeNH**]BF_4 with excess $[Et_4N][BF_4]$ in CD_2Cl_2.

Positive phase data in 2D NMR spectra are depicted as red, and negative phase data are depicted as blue.

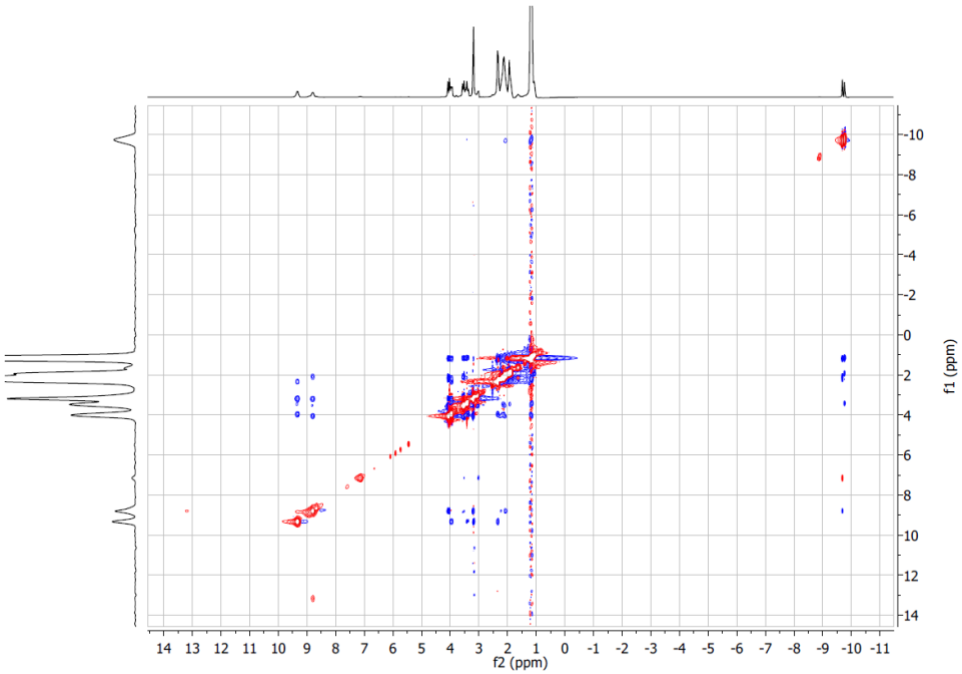

Figure S14. 300 MHz $^1H\{^{31}P\}$ NOESY NMR Spectrum of [**FeHNH**][OTf]$_2$ in CD_3CN at −40°C.

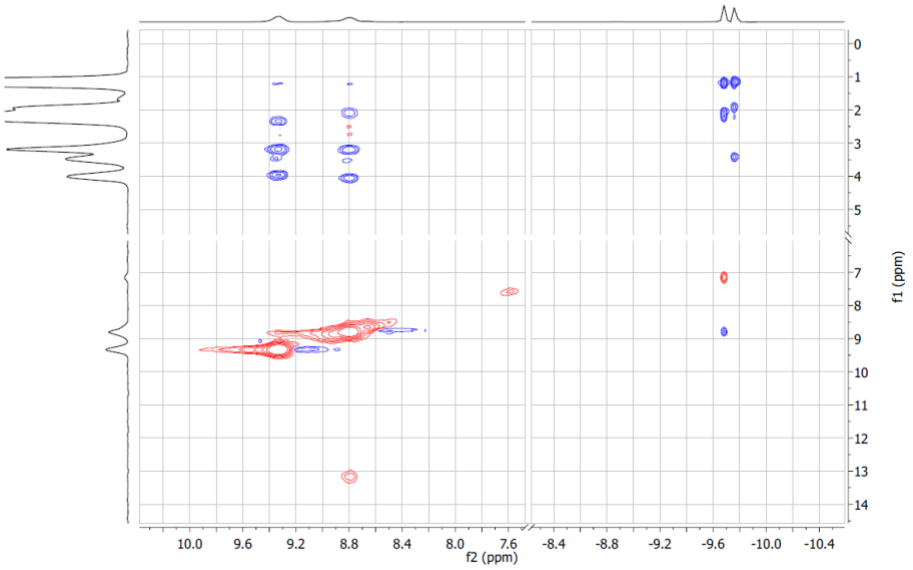

Figure S15. 300 MHz $^{1}H\{^{31}P\}$ NOESY NMR Spectrum of [**FeHNH**][OTf]$_2$ in CD_3CN at −40°C magnifying the areas showing exchange correlations (positive phase) and NOESY correlations (negative phase) between the NH protons and FeH protons.

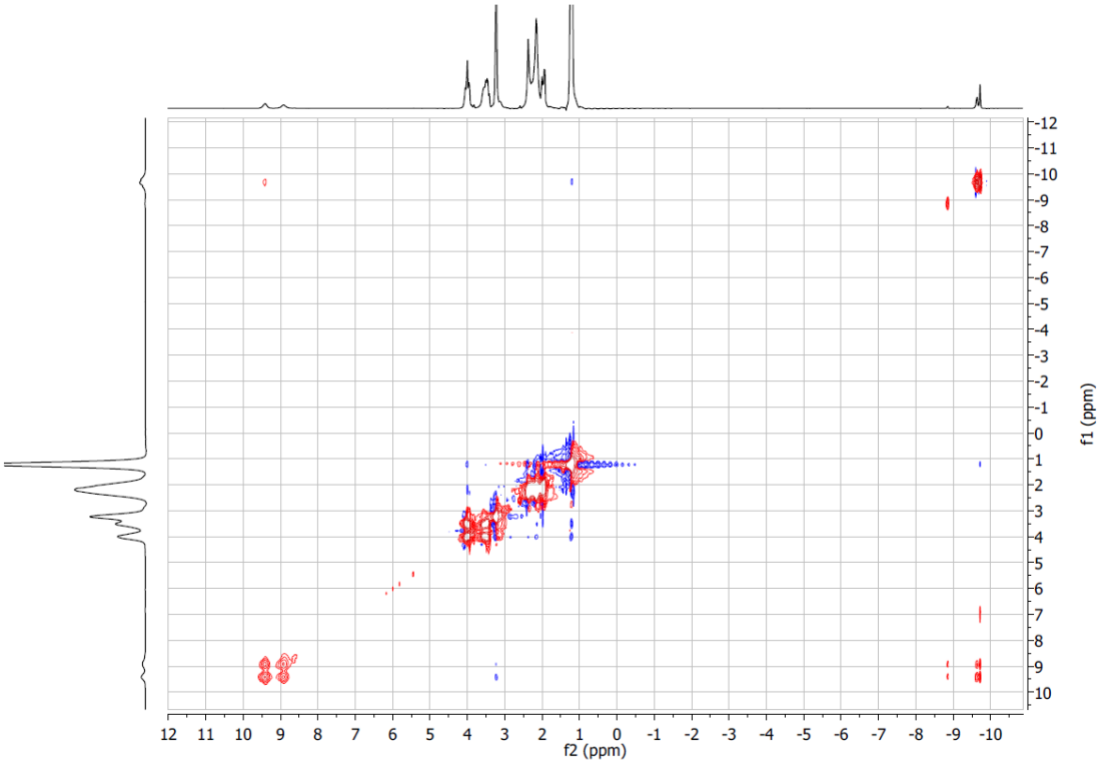

Figure S16. 300 MHz $^{1}H\{^{31}P\}$ NOESY NMR Spectrum of [**FeHNH**][OTf]$_2$ in CD_3CN at +25°C.

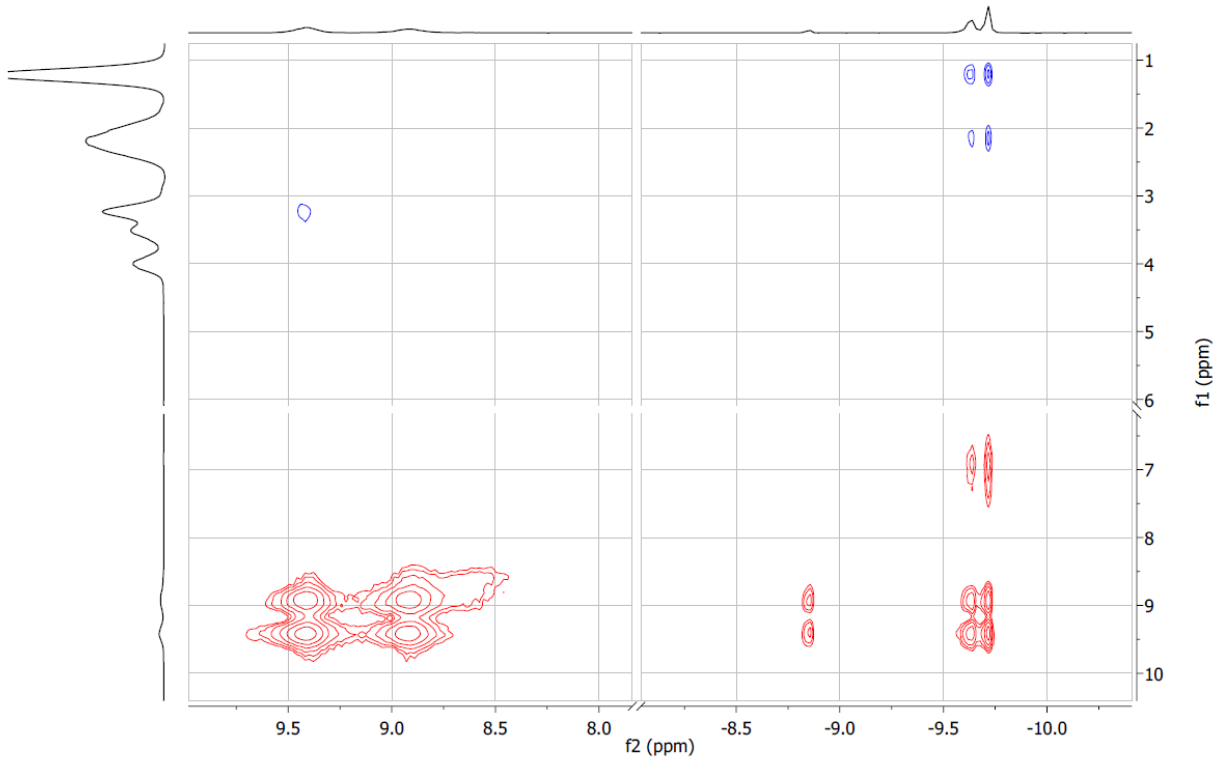

Figure S17. 300 MHz $^{1}H\{^{31}P\}$ NOESY NMR Spectrum of [**FeHNH**][OTf]$_2$ in CD_3CN at +25°C magnifying the areas showing exchange correlations (positive phase) and NOESY correlations (negative phase) between the NH protons and FeH protons.

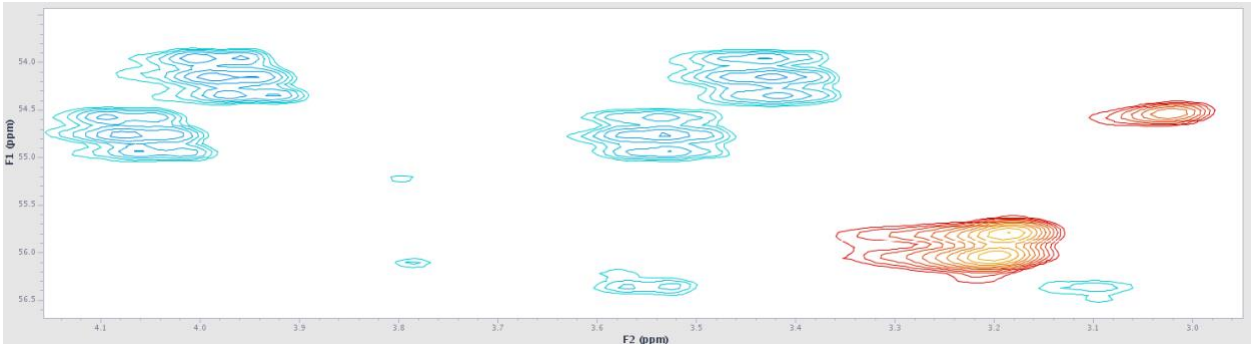

Figure S18. 300 MHz ^{1}H-^{13}C HSQC NMR Spectrum of [**FeHNH**][OTf]$_2$ in CD_3CN at −40°C magnifying the areas with CH_3 correlations (positive phase) and CH_2 correlations (negative phase). Three distinct CH_3 carbons can be discerned. Three distinct CH_2 carbons of approximate equal intensity and one CH_2 carbon of weaker intensity can be discerned.

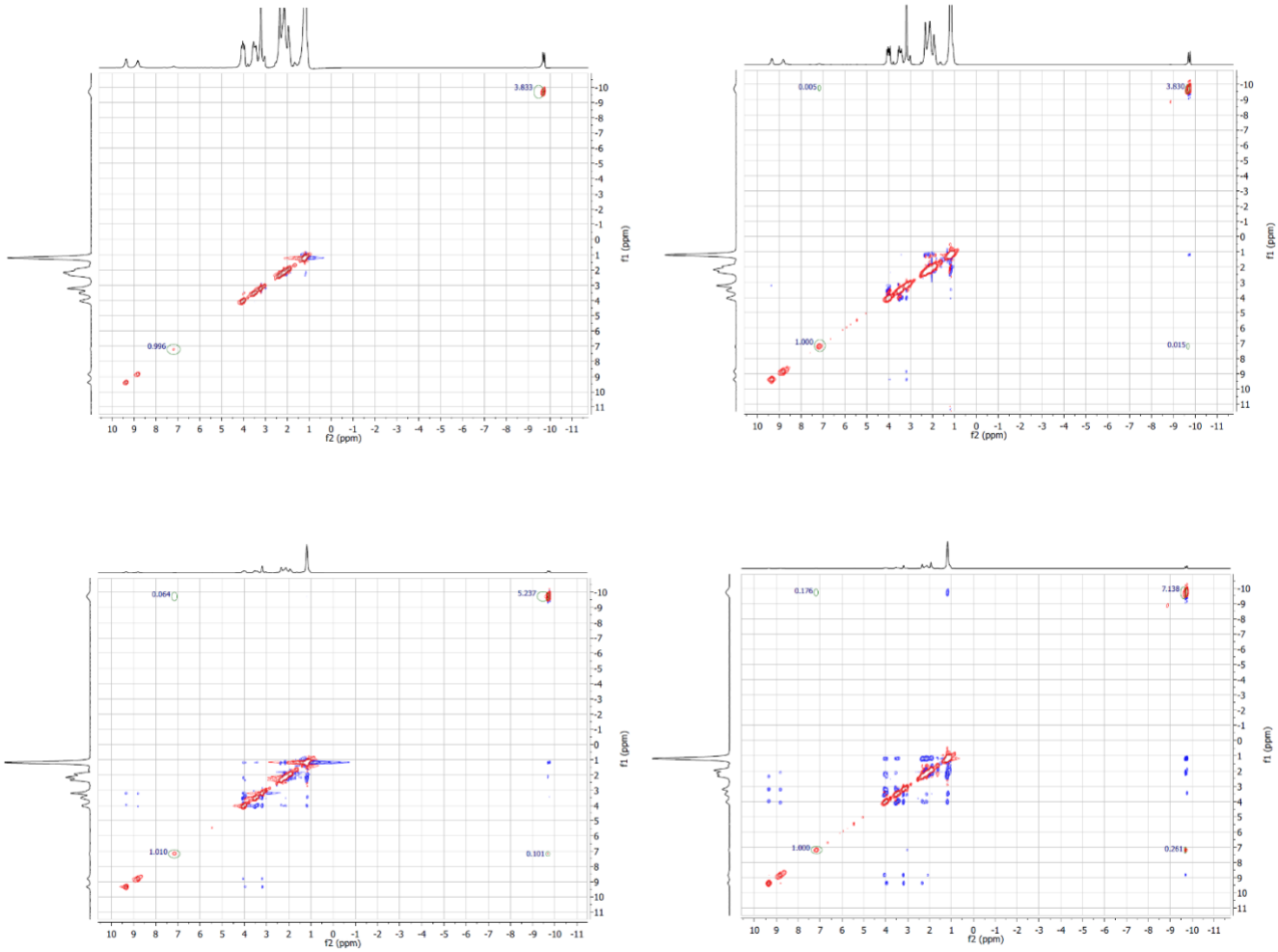

Figure S19. ^{1}H NMR NOESY Spectra of [**FeHNH**][OTf_2] in CD_3CN at −40°C at various mixing times (T_m). (Top Left) T_m = 0 ms. (Top Right) T_m = 50 ms. (Bottom Left) T_m = 200 ms. (Bottom Right) T_m = 500 ms.

Infrared Spectra

Table S1. Summary of Diagnostic $\tilde{\nu}_{CO}$ IR Data in CH_2Cl_2 Solution

Complex	$\tilde{\nu}_{CO}$ **(cm^{-1})**
Fe^0	1976, 1900, 1873
Fe(P^{Et}N^{Ph}P^{Et})(CO)$_3$	1978, 1903, 1877
[Fe^I]$^+$ [BAr$^F{}_4$]$^-$	2069, 2007, 1999
[Fe(P^{Et}N^{Ph}P^{Et})(CO)$_3$]$^+$ [BAr$^F{}_4$]$^-$	2070, 2008, 1999
[FeH]$^+$ [B(C$_6$F$_5$)$_4$]$^-$	2089, 2033
[FeNH]$^+$ [BF$_4$]$^-$ (KBr pellet)	1993, 1933, 1890
[Fe(P^{Et}N^{Ph}P^{Et})(CO)$_3$H]$^+$ [B(C$_6$F$_5$)$_4$]$^-$	2090, 2035
[FeH(CO)$_3$(depp)]$^+$BF$_4^-$	2086, 2064
[FeHNH]$^{2+}$ [OTf]$_2$	2100, 2049

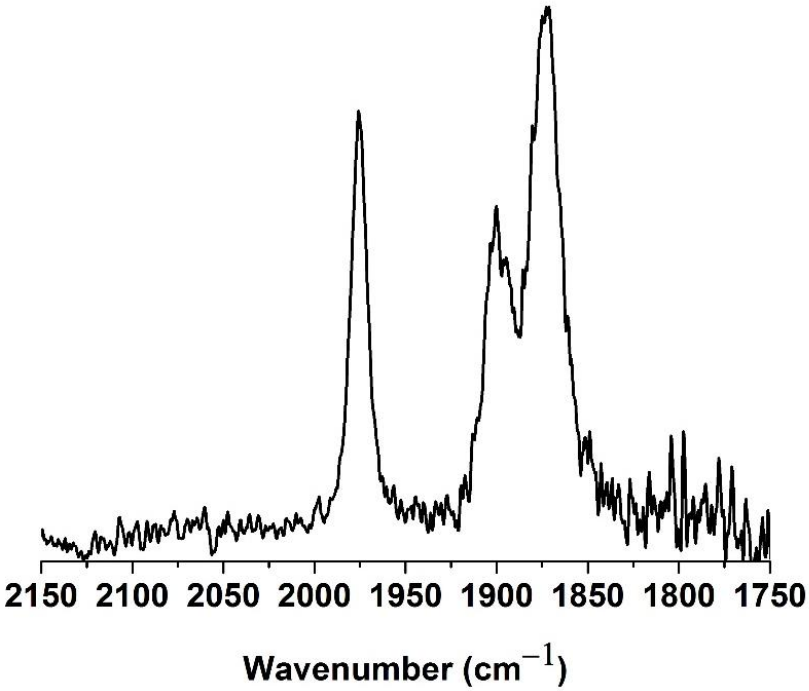

Figure S20. IR Spectrum of **Fe^0** in CH_2Cl_2 solution.

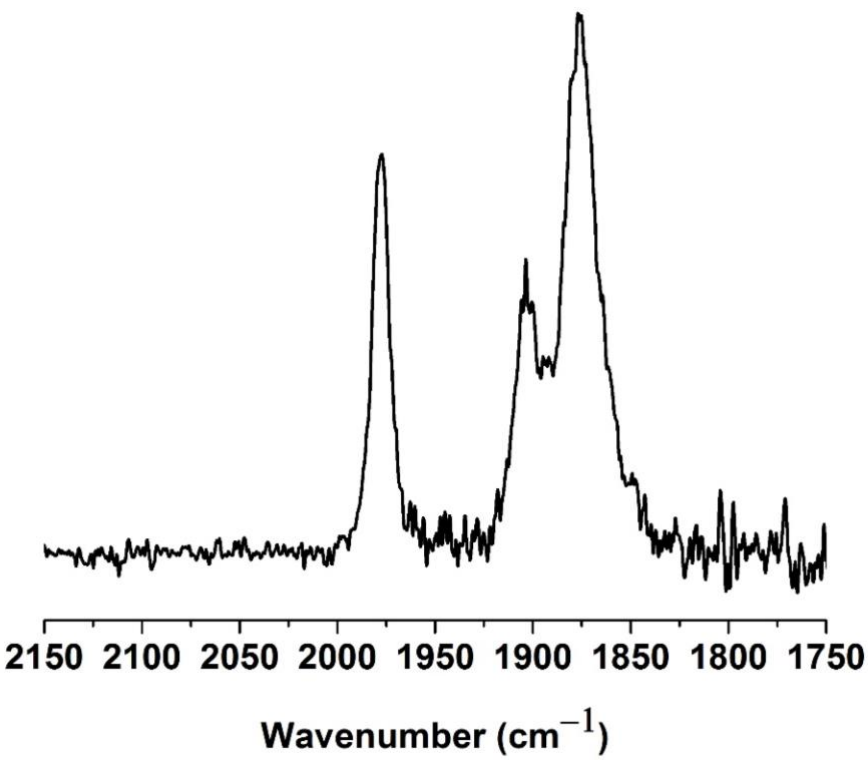

Figure S21. IR Spectrum of **Fe(P^{Et}N^{Ph}P^{Et})(CO)$_3$** in CH_2Cl_2 solution.

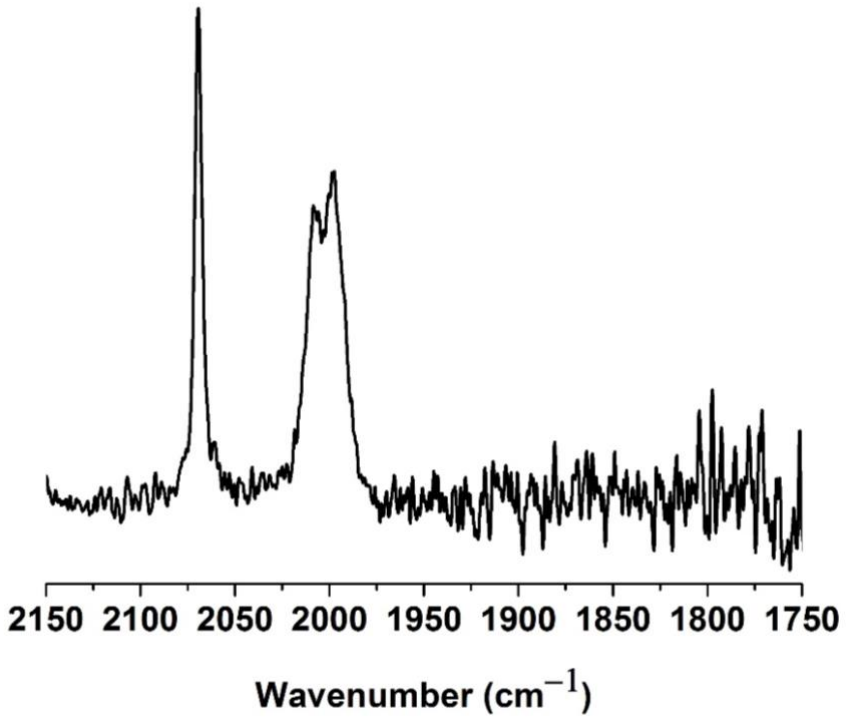

Figure S22. IR Spectrum of [**Fe^{I}**][B(C_6F_5)$_4$] in CH_2Cl_2 solution.

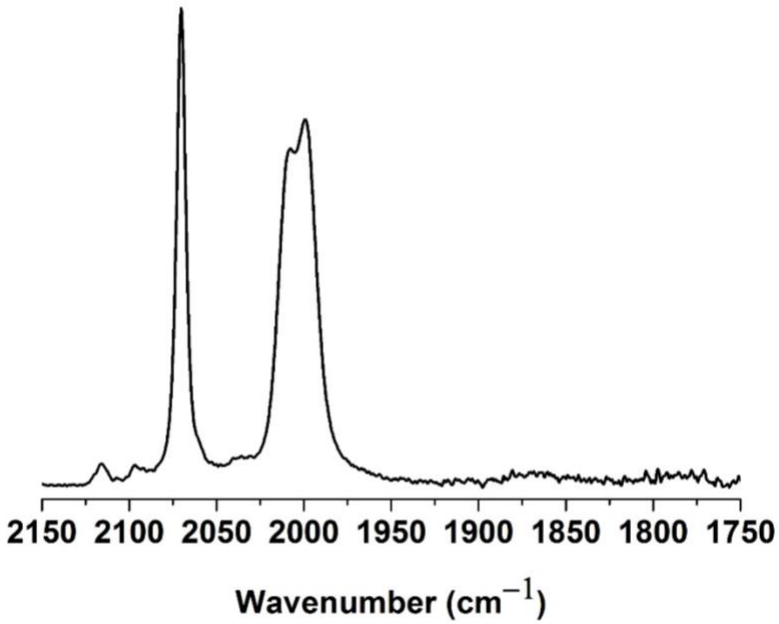

Figure S23. IR Spectrum of **[Fe(P^{Et}N^{Ph}P^{Et})(CO)$_3$]**[BAr$^F{}_4$] in CH_2Cl_2 solution.

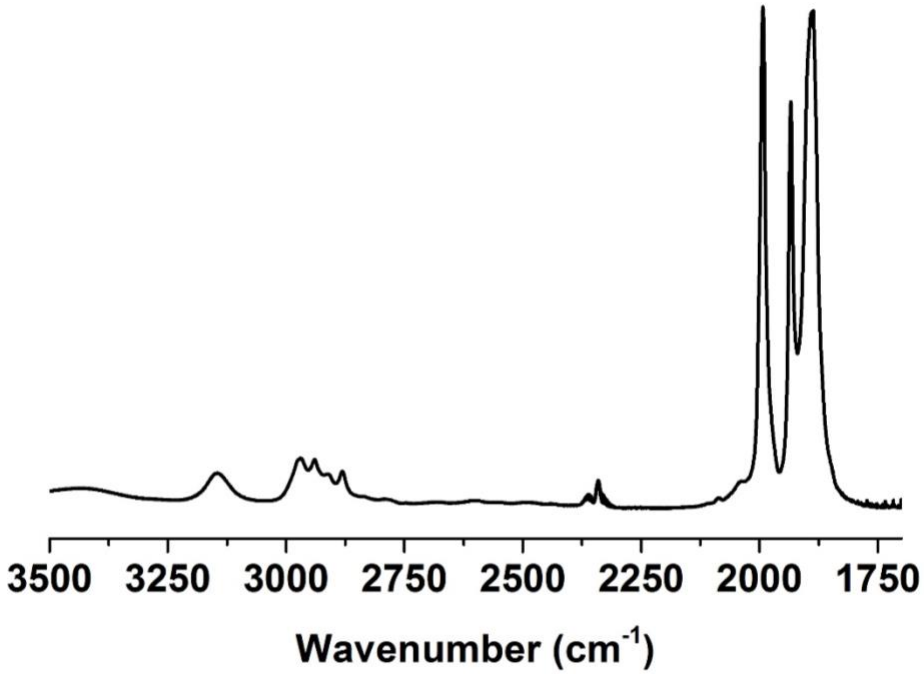

Figure S24. Solid state IR (KBr) of crystalline of the amine protonated tautomer [**FeNH**][BF_4]. Bands (cm^{-1}): $\tilde{\nu}_{NH}$ = 3142 (br), $\tilde{\nu}_{CO}$ = 1993, 1933, 1890 (br).

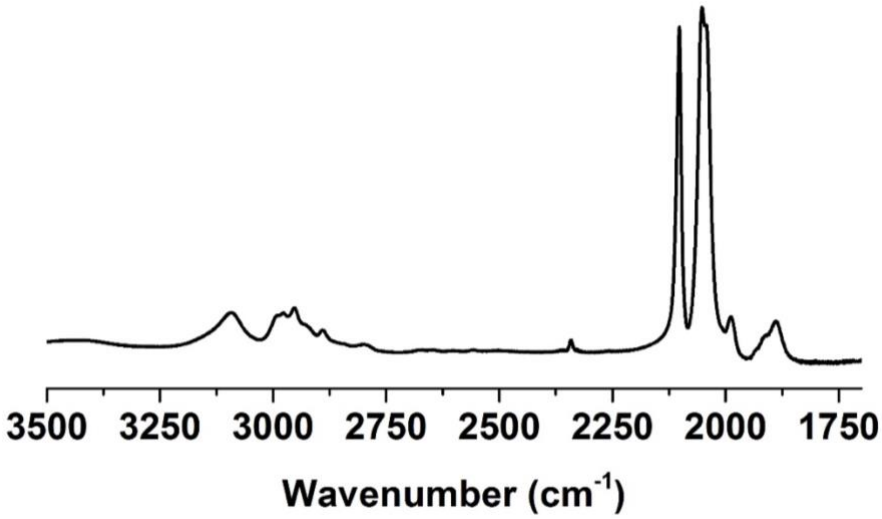

Figure S25. Solid state IR (KBr) of crystalline of [**FeHNH**]$^{2+}$[OTf]$_2$. Bands (cm^{-1}): $\tilde{\nu}_{NH}$ = 3142 (br). $\tilde{\nu}_{CO}$ = 2103 (m), 2042 (s, br) cm^{-1}.

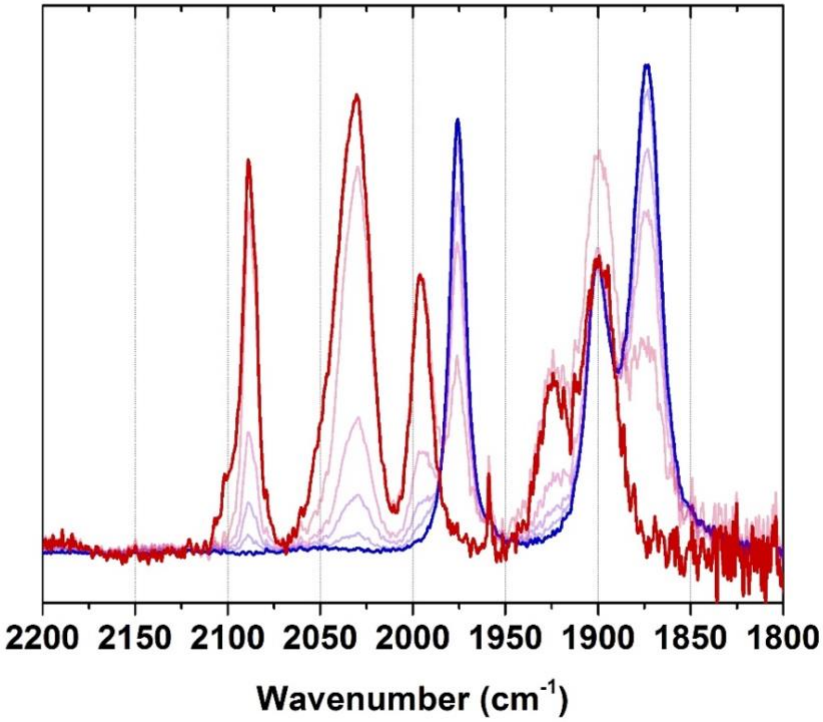

Figure S26. IR Spectrum of **Fe^0** (blue trace) treated with increasing amounts of $HBF_4 \cdot Et_2O$ up to 1 equiv. (red trace). Two sets of bands grow in as increasing amounts of acid are added; the higher energy bands correspond to the iron protonated tautomer [**FeH**]$^+$ and the lower energy bands correspond to the nitrogen protonated tautomer [**FeNH**]$^+$

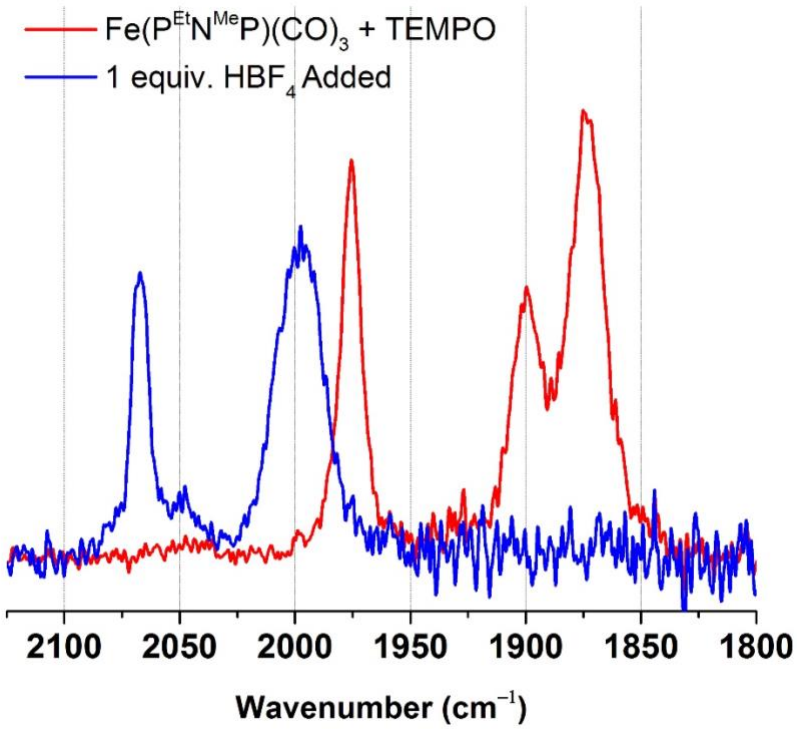

Figure S27. (Red trace) IR spectrum of **Fe^0** in CH_2Cl_2 solution with one equivalent of TEMPO showing no reaction between TEMPO and **Fe^0**. (Blue trace) IR spectrum of the previous solution treated with 1 equiv. HBF_4 •OEt_2 showing formation of IR bands corresponding to [**Fe^I**]$^+$

Electrochemical Data

Unless otherwise noted, electrochemical data were collected in PhF using $[Bu_4N][B(C_6F_5)_4]$ as the supporting electrolyte, glassy carbon as the working electrode, a silver wire as a pseudo reference, and a platinum wire as the counter electrode under argon.

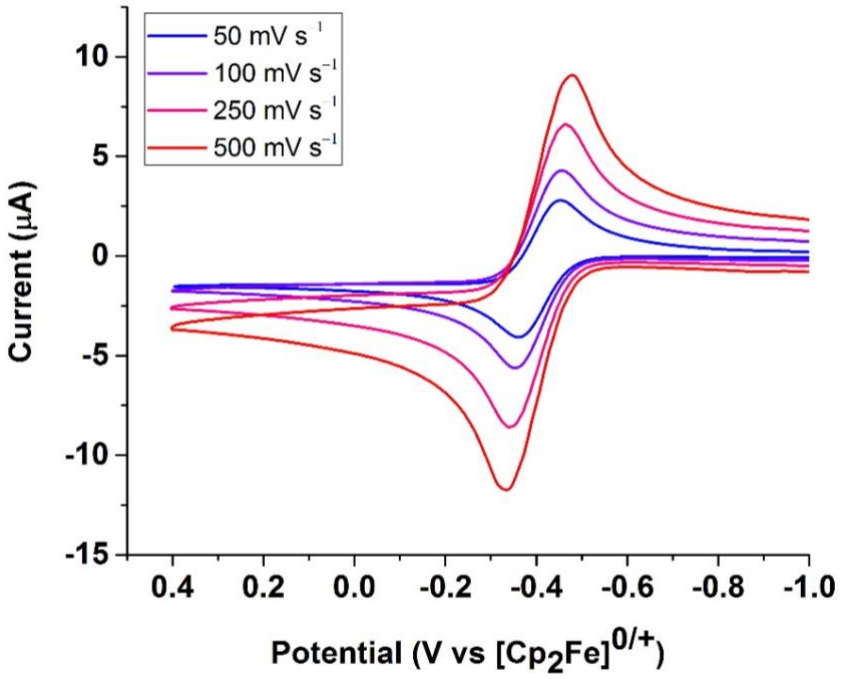

Figure S28. CV of **Fe^0** at variable scan rates in PhF.

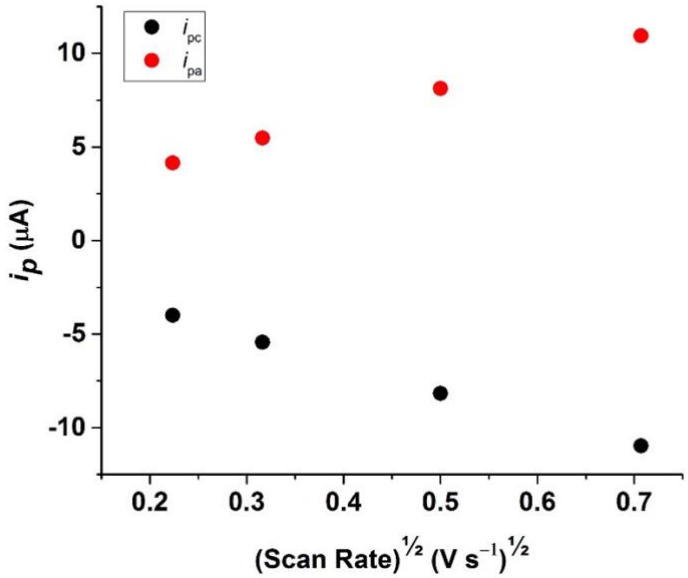

Figure S29. Plot of i_p vs (scan rate)^{½} from CV traces in Fig S32. showing a linear relationship indicating a diffusion-controlled process.

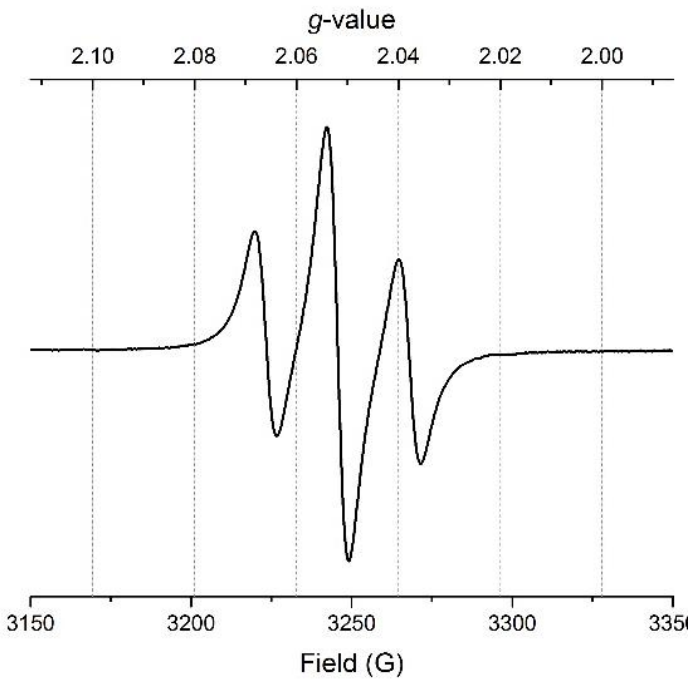

Figure S30. X-band EPR spectrum of [**Fe^{I}**]$^{+}$[BAr$^{F}{}_{4}$]$^{-}$ in Et_2O solution at 22 °C.

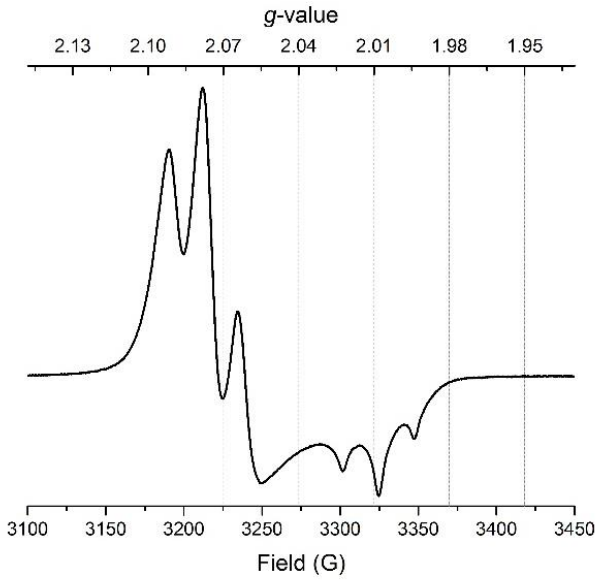

Figure S31. EPR spectrum of [**Fe^{I}**]$^{+}$[BAr$^{F}{}_{4}$]$^{-}$ in Et_2O at 77K.

Computational Methods

Density functional theory was used to optimize geometries, calculate energetics and calculate wavefunctions for use in Natural Bond Orbital (NBO) analysis. The BP86 functional[14-16] modified by the Becke-Johnson damped D3 correction[17, 18] was used because of its previous use for predicting protonation at ligand vs. metal and its ability to capture noncovalent hydrogen bonding interactions.[19] A large 6-311++G** basis set was used on all atoms[20, 21] with the Stuttgart-Dresden ECP applied to Fe.[22] Geometry optimizations were followed by frequency calculations to correct for zero-point vibrational energy. Free energies were calculated at 298.15 K using the modified harmonic oscillator approximation wherein low-lying vibrational frequencies are treated as free rotors.[23] Single point solvation energies in continuum dichloromethane solvent were calculated at the same level of theory using the SMD model.[24] These calculations were completed in ORCA 4.0.[25] Subsequent NBO analysis was completed in the standalone NBO 6.0 program[26] from wavefunctions calculated at the 6-31G* basis set.[27]

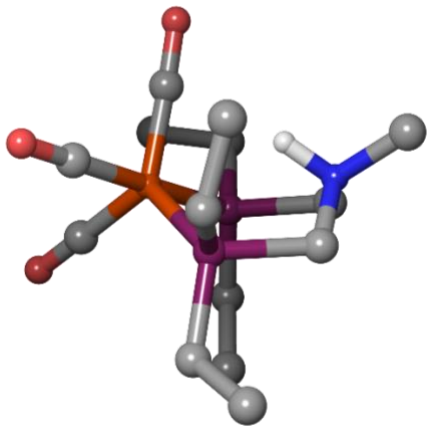

Figure S32. Structure of the "tucked in" conformation of **[FeNH]**$^{+}$. Additional hydrogens omitted.

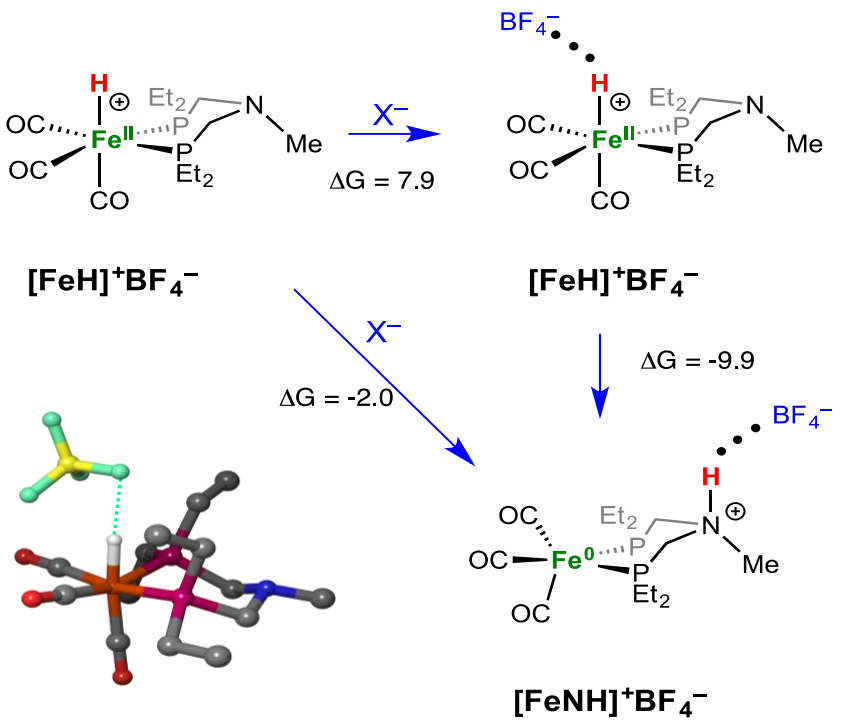

Figure S33. The interaction of BF_4^- with the protonated amine is more favorable than the interaction with the metal hydride. Additional hydrogens omitted

Detailed NBO analysis

Key: LP– lone pair; CR– core; BD– bonding; BD*– antibonding

Table S2. Interactions with N–H bond in **[FeNH]$^+$BF$_4^-$**.

Interactions	q_{CT}	$E^{(2)}_{\sigma\sigma^*}$ [kcal/mol]
LP F53 → BD* N-H	0.0180	11.6
CR F53 → BD* N-H	1.34E-05	0.2
B-F53 → BD* N-H	0.0035	2.7
LP F46 → BD* N-H	0.0002	0.1
B-F46 → BD* N-H	0.0002	0.1
total q transfer	0.0220	14.8

Table S3. Interactions with N–H bond in **[FeNH]$^+$OTf$^-$**

Interactions	q_{CT}	$E^{(2)}_{\sigma\sigma^*}$ [kcal/mol]
LP O51 --> BD*(N-H)	0.0391	19.6
BD S-O51 --> BD*(N-H)	0.0007	0.5
CR O51 --> BD*(N-H)	8.87E-06	0.1
total q transfer	0.0399	20.3

Table S4. Interactions with N–H bond in **[FeNH]$^+$CH$_2$Cl$_2$**

Interactions	q_{CT}	$E^{(2)}_{\sigma\sigma^*}$ [kcal/mol]
LP Cl46 → BD N47-H48	0.000435	0.2

Table S5. Interactions with Fe–H bond in **[FeNH]$^+$BF$_4^-$**.

Interactions	q_{CT}	$E^{(2)}_{\sigma\sigma^*}$ [kcal/mol]
LP H54 --> B–F2	0.0047	0.7
LP H54 --> B–F3	0.0027	0.5
LP H54 --> B–F4	0.0081	1.5
LP H54 --> B–F5	0.0023	0.4
total	0.0177	3.0

Interactions in the Dicationic Complex – Dihydrogen Bonding

Similar computational studies can be done to quantify dihydrogen bonding in the dication [**FeHNH**]$^{2+}$. The structure of the boat isomers of the dication with and without counterion present were calculated. In these calculations, a single BF_4^- is used for simplicity. In the structure of [**FeHNH**]$^{2+}$, the H–H distance is 1.72 Å (Figure S34a). In the structure of [**FeHNH**]$^{2+}$[BF_4^-], the H–H distance lengthens to 2.16 Å (Figure S34b). The counterion positions itself in between the two H atoms, with an N–H…FBF_3 distance of 1.51 Å and a Fe–H•••FBF_3 distance of 2.24 Å. The lengthening effect on the hydrogen-hydrogen distance is consistent with calculations on [FeFe]-hydrogenase models.[28] To probe the existence of a dihydrogen bond, NBO calculations were used to search for interactions between the Fe–H bonding orbital and the N–H antibonding orbital. In [**FeHNH**]$^{2+}$, there is 5.7 kcal/mol of stabilization energy ($E^{(2)}_{\sigma\sigma^*}$), implying the existence of a dihydrogen bond. However, that stabilization is weakened to 2.9 kcal/mol in the presence of counterion in [**FeHNH**]$^{2+}$[BF_4^-]. For comparison, a stabilization energy of 16.1 kcal/mol is computed between the N–H bond and the BF_4^- counterion, suggesting that much more stabilization comes from the interaction with the counterion.

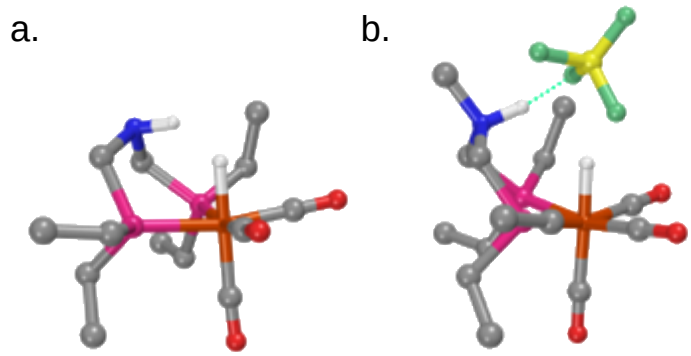

Figure S34. The dication (a) without, and (b) with stabilization by a counterion, though the counterion increases the distance between the relevant protons. Additional hydrogens omitted for clarity.

Geometries of computed complexes

The following geometries are in XYZ format and can be opened with any chemistry-based viewer.

49

[FeH]$^+$

Fe	-0.04473540800546	-1.08900810055966	0.68175706226391
P	2.04108048187517	-0.88640701546278	-0.20434763666417
P	-0.99210172042328	-0.44125851294751	-1.28016750977654
O	-0.16305600172885	-3.97291638357924	0.00576435160781
O	1.21212463047441	-1.21600519345876	3.33597410405358
O	-2.68886032514888	-0.69329738103893	1.90482948385738
N	1.32836178244770	-0.53069202849612	-2.84141154952079
C	-0.12449538292989	-2.84923469402185	0.26953875215216
C	0.72489767745491	-1.19520925795536	2.29152788822046
C	-1.65912491389308	-0.87487502076538	1.41935790937710
C	-2.67931847589493	-1.13875844612213	-1.62440066186436
H	-3.37055758398256	-0.60442039474565	-0.95277695924905
H	-2.92990380277514	-0.81114633435444	-2.64828367118631
C	-2.85296650873845	-2.65263428887930	-1.48121282270858
C	-1.34107703003103	1.36588383064938	-1.46451857468224
H	-1.90188254343116	1.46161885641658	-2.41015827047449
H	-2.04473415064389	1.61282244293893	-0.65219797672034
C	-0.13966080645589	2.31138636131870	-1.44909889228442
C	3.35134487148204	-1.91135141158180	0.61399180651134
H	4.26649883761291	-1.74530174748739	0.02000264231229
H	3.53215116657464	-1.44544006924266	1.59619318933387
C	3.06674702251367	-3.40705506510123	0.77285225937190
H	2.21542624943428	-3.59432206478603	1.44097479863523

H	3.94307842827457	-3.90086162458869	1.21725067567408
H	2.86440188122340	-3.89948884904766	-0.18890452257591
C	2.80641303901350	0.79244234062273	-0.22621754523903
H	3.85422764455469	0.63443699190841	-0.53401941558076
H	2.31001049102041	1.34017918363916	-1.03854694076108
C	2.73593521836634	1.55185657631947	1.10147666910905
H	1.69383615672359	1.74530896333970	1.39771002344693
H	3.24241233330886	2.52266668257131	1.00637311779713
H	3.22441830907368	1.00325644035930	1.92033026707919
C	2.15596197642714	-1.38494995223863	-1.99100236037590
H	3.21159204506600	-1.24809507591030	-2.27405174126510
H	1.91914893821847	-2.46656142564775	-2.08929867211139
C	-0.07877840078063	-0.92502990671066	-2.82514826028348
H	-0.22239334396294	-2.01906929937013	-2.97677573483698
H	-0.59976502018017	-0.40865237238748	-3.64712067598618
C	1.84581107231792	-0.48467568535501	-4.22057859996896
H	1.81587850314801	-1.47382721478002	-4.72250792912546
H	2.88451302077426	-0.12636157615496	-4.20539141051824
H	1.24875491994716	0.22674982575711	-4.80843154430893
H	0.36378638534893	2.29986428700467	-0.47235671328908
H	-0.47723446637855	3.34175482057929	-1.63281112366406
H	0.59066891114329	2.04155674370250	-2.22435604449223
H	-3.86562767804372	-2.93568826959202	-1.80306743031995
H	-2.74055110709274	-2.98023478553890	-0.43942795591846
H	-2.14275803771242	-3.21895702105824	-2.09993142993987
H	0.09570071441372	0.40810212183945	0.87261557488891

49

[FeNH]$^{+}$

Fe	0.47285802353718	1.21555342923927	-0.63144730033874
P	1.27057034293033	0.68410227403920	1.35897153278010
P	-1.68512212744140	1.00234111291248	-0.13449220119005
O	3.21550252659803	1.65418214758439	-1.57635028530432
O	-0.11991144501917	4.06083041475075	-1.07832788890147
O	0.10103970601580	-0.81116762663296	-2.73045835684421
C	2.90221951588528	-0.21384976098534	1.37485081773616
H	3.65568920416141	0.51889883829755	1.04448264969985
H	3.14497162022748	-0.47640630819552	2.41664706236710
C	0.24393252628980	-0.02346107627721	-1.87790206152103
C	2.93375994432017	-1.45435719252740	0.47717760103780
H	2.69006354947752	-1.20908216111748	-0.56568282964075
H	2.22538246416025	-2.22884143053585	0.81799544621709
H	3.93351642819115	-1.91217599299739	0.49274677924692
C	1.49490724856151	1.94471979779678	2.70127560593707
H	2.22716351166012	2.65752297660368	2.28489178437698
H	0.54575437687575	2.49413474022347	2.76055795809342
C	0.12318587545674	2.93743585916009	-0.89227794131937
C	0.17934792111811	-0.62340519653848	2.19941439147503
H	0.79608327853480	-1.40895178223869	2.65359745198537
H	-0.47580044410384	-0.19096872279335	2.96645916953284
C	2.13460306437118	1.47530435505742	-1.19624769245817
C	1.93334358358687	1.43897291380455	4.08111325529030
H	2.91979262373268	0.95544407244262	4.05437547332156
H	1.21293473141069	0.72510912528285	4.51148774708202
H	2.00646927426656	2.28461409434234	4.78109139704421

C	-0.86338828301906	-2.73987973343258	1.31721048400901
H	0.12531687918384	-3.21207856030412	1.37159644914856
H	-1.41558233296827	-3.13711851651117	0.45619943784007
H	-1.42290821121076	-2.92126185914170	2.24321629849838
C	-1.98973486598648	2.85113517132928	2.03369581309940
H	-1.77437506103702	2.05422039213956	2.76414747568440
H	-2.65917053117473	3.57194653945880	2.52592693432112
H	-1.05250786554323	3.37327116094341	1.79905980556148
C	-2.80631006660055	0.63727849795980	-1.56719073340979
H	-2.50667780721329	-0.34661065949672	-1.96234956171733
H	-3.83394324604011	0.54088335436865	-1.17561457956481
C	-2.64220806708971	2.31141610457070	0.76137620680525
H	-2.77959755874102	3.12502529527576	0.03218701006034
H	-3.64320503140797	1.89301277324641	0.96150344678798
C	-2.72469147827970	1.69983629184427	-2.66954617828569
H	-3.37715659054082	1.41770563216909	-3.50770267731512
H	-1.69899464931983	1.79283849498580	-3.05197179923782
H	-3.04928072250043	2.68848191203483	-2.31502205685267
N	-0.67928314238254	-1.26545903845762	1.13099689452518
H	-0.13979972601411	-1.06254555832921	0.23069516297762
C	-1.98033191367874	-0.52777350645368	0.94223159930831
H	-2.38764851902679	-0.27816883780874	1.93072708198858
H	-2.67647853421371	-1.19925425108859	0.42247792006184

54

[FeNH]$^{+}$ BF$_4^{-}$

Fe	0.42408645794182	1.59697827074599	-0.73978793430006
P	1.63026444528513	0.53514945787438	0.75706530963257
P	-1.50960234520152	1.13173962230997	0.24917768949054
O	2.90379593897431	2.36806465939127	-2.09294888381581
O	-0.12477882121259	4.46237610057119	-0.39730066492584
O	-0.35404815032263	0.09662680310171	-3.14832068614792
C	3.15188208201864	-0.34593954275339	0.15178794563536
H	3.83502199089827	0.44635906444883	-0.19585303666928
H	3.63658091232011	-0.83215177501240	1.01577234769066
C	-0.05479979846001	0.64459171607452	-2.16453597165128
C	2.86179242166319	-1.34954294988619	-0.97036057356141
H	2.39481982528478	-0.85315141157566	-1.83192547345278
H	2.18864914285747	-2.15488089876257	-0.64481145700792
H	3.79979387788131	-1.81237584601335	-1.31133240881038
C	2.34538726482636	1.59198842385354	2.11778397316922
H	2.97901854189446	0.96897239442434	2.77367044262181
H	3.00848933376551	2.30572455626013	1.60237678236858
C	0.08410113787636	3.31441553825332	-0.50438480952605
C	0.90128419473652	-0.85211128751996	1.80988215139624
H	1.45082489093870	-1.77707118430824	1.59139189514376
H	1.01125855196386	-0.60406146460288	2.87710137453697
C	1.91819939765339	2.05406710821524	-1.55603242030076
C	1.28181619084684	2.34524988570272	2.91850987517790
H	0.64196992690037	1.65803571488512	3.49812498408790
H	0.63634783766906	2.92731396668208	2.24296057213025
H	1.74377302103557	3.03962689488768	3.63610166227259

C	-0.95825664706108	-2.29739162336028	2.50474219599324
H	-0.25392582773716	-3.12555946202290	2.37462467199468
H	-1.95709533813713	-2.63805443417368	2.20958377850584
H	-0.95426399923114	-1.91774927376250	3.53551921078242
C	-3.72072699844863	2.23362576285258	1.77207728009886
H	-4.45471929263470	1.76973491020998	1.09714463694213
H	-4.17046096967751	3.16206350544387	2.15555329578501
H	-3.58072754173773	1.56395732896668	2.63401675746095
C	-2.83019819874086	0.32750971625044	-0.77936127382442
H	-2.37398394151582	-0.56841050636175	-1.22608914777945
H	-3.63914133743745	-0.01874649309157	-0.11502613995103
C	-2.40315243041158	2.55184924983742	1.05682078245819
H	-1.67666924758603	3.01518508369068	1.74321733622403
H	-2.56184542187733	3.28623099394658	0.25308567374895
C	-3.37396983801998	1.27172149520204	-1.85798181014622
H	-4.06073800635783	0.72704734485876	-2.52263834003152
H	-2.56406641886260	1.67994376141400	-2.47898547662696
H	-3.92749031327570	2.11675112034325	-1.42060978027598
B	-0.50679959345366	-3.67247114395580	-0.54372186274201
F	0.64235383918651	-3.62562474280430	0.31615184372320
N	-0.54401164265063	-1.18543802599358	1.58345448840069
H	-0.63029681743931	-1.56840917421480	0.58433237828162
C	-1.45753271314720	-0.00874359861550	1.73783203918120
H	-1.13472401022032	0.55997588704369	2.62326842881595
H	-2.46712448067271	-0.40248717872825	1.91875366433611
F	-1.59085307594352	-4.22790952864421	0.15339350093020
F	-0.85167604382458	-2.23353146037320	-0.78144898822613
F	-0.23393196311957	-4.27656333120499	-1.74702182924444

57

[FeNH]$^{+}$OTf^{-}

Fe	0.30985746753601	1.55875880740517	-0.64514446401657
P	1.61597243483018	0.90278498211377	0.97588640827831
P	-1.55454780453870	1.19713419203236	0.51069861509368
O	2.72185589591401	2.19721109869246	-2.17931807076082
O	-0.52696275290631	4.35479640215805	-0.96372288388389
O	-0.44365150440386	-0.40059176802229	-2.70673186164925
C	3.06434514989694	-0.17131683826674	0.49929951223184
H	3.74860055776608	0.48654951737388	-0.06269116874774
H	3.59644373230808	-0.48012215710291	1.41455114396514
C	-0.16257054434542	0.32555827720009	-1.84199355799826
C	2.66902092679477	-1.38494620263997	-0.34644537627871
H	2.17742294725279	-1.07481929818719	-1.27740294165658
H	1.96401991780500	-2.05085190051311	0.17322081715232
H	3.56170680216190	-1.97400637182518	-0.60585646364755
C	2.43750810661125	2.26524092977895	1.95134316243796
H	2.90121119618367	2.90800645687050	1.18503572657668
H	1.60732455296211	2.85609848146884	2.37087065007651
C	-0.19388828936322	3.24247268989538	-0.80453065098940
C	0.92209661004568	-0.09974227829952	2.40936067348529
H	1.67413065163184	-0.83545510439755	2.72387154835890
H	0.71397668893962	0.56754727122431	3.26066739261462
C	1.75974420325164	1.93909993745812	-1.57180738766096
C	3.45635033091520	1.87909677696357	3.03200025190617
H	4.32509279996057	1.35738831556615	2.60579107927218
H	3.02093414446003	1.23002461622168	3.80860343732958
H	3.83271075131792	2.78137970833986	3.53800004136269

C	-0.57699105300389	-1.88119565463048	3.19286086023210
H	0.27270925343155	-2.57559746389825	3.20112762705956
H	-1.49660877389349	-2.42312716518755	2.93903507892165
H	-0.66437217160585	-1.37208113992160	4.16286889583324
C	-1.35046765457153	3.38655216613219	2.33161879539897
H	-1.00640000956550	2.73540287920028	3.15181321380305
H	-1.84736244256164	4.25395519139756	2.79096443647174
H	-0.46457408580526	3.74999942734937	1.79282737421709
C	-2.99527087692427	0.54406652512760	-0.45534889760418
H	-2.69581109976303	-0.43144312212469	-0.86590196802866
H	-3.82888160924418	0.36122128613142	0.24246232995727
C	-2.30582078960379	2.66262389908406	1.38003427649672
H	-2.63887303800741	3.34812389769144	0.58649088258961
H	-3.20976548586585	2.30914400338662	1.90505212793488
C	-3.41008224297203	1.48840287626317	-1.59033829841108
H	-4.17672553829561	1.00315227160464	-2.21209840101761
H	-2.55482772814183	1.73183353937466	-2.23750426418671
H	-3.83150814762353	2.43163550245512	-1.21172795527568
N	-0.33606456715561	-0.85714005242045	2.12266018880146
H	-0.26862654742991	-1.42927227815424	1.18756096107750
C	-1.53617966469667	0.02832136134394	1.99124060586004
H	-1.61461114434897	0.61172179382249	2.92121960535526
H	-2.39938152712636	-0.64683085139321	1.89876306043788
S	-1.82447374217868	-3.00980271260918	-0.10037730742931
O	-0.43900935595554	-2.38152887509715	0.02327432550725
O	-2.44120146548403	-2.87126626370544	-1.42938739201051
C	-1.42064641397618	-4.85312483966755	0.10015669120509
F	-0.58910330232407	-5.27273613087920	-0.87241405314162

F	-0.81476143256024	-5.06449593052896	1.30036605186426
F	-2.54737854273816	-5.59121147694119	0.05962093565635
O	-2.68443377299625	-2.69889920471409	1.08372457957224

54

[FeNH]$^+$ CH_2Cl_2

Fe	0.26235116074577	1.36801638319594	-0.87672554876922
P	1.52168587851065	0.69812455784120	0.79069123695408
P	-1.63839692699299	1.07602920392074	0.22470871036645
O	2.70295348897867	1.73657384511658	-2.46085102220800
O	-0.29378304196481	4.25438840206057	-0.94629377873657
O	-0.84188325186205	-0.24016840525250	-3.07004535894808
C	3.02478349567587	-0.32196356853080	0.38358355078003
H	3.68986645304456	0.34562693710571	-0.18761087450039
H	3.54611328809292	-0.56211146565186	1.32571941557474
C	-0.39217966783632	0.34982374597390	-2.16719289360732
C	2.71465820018362	-1.58234445629330	-0.42557108034876
H	2.16201177348932	-1.34220055798547	-1.34534917774747
H	2.11951333902208	-2.31153997343498	0.14902124544301
H	3.64331394750241	-2.09617735501763	-0.71231229140787
C	2.27521534225962	1.90235259964105	1.99244634963146
H	2.81308307279545	1.33317951606641	2.76988018876431
H	3.04352611077127	2.42257751391452	1.39548871601449
C	-0.06903257878629	3.11192270800642	-0.89687819076437
C	0.64175552422427	-0.47048050390161	1.97882174543408
H	1.35337703104126	-1.18168952983677	2.41897847749805
H	0.13836515550870	0.07726886462437	2.78625615582487
C	1.73898246864722	1.59200014058466	-1.83027322599581
C	1.30959822202700	2.91668826346397	2.60169036241566

H	0.57302506446589	2.43679622778573	3.26591791145820
H	0.76697816658944	3.46513065606500	1.81943671989233
H	1.86009105563163	3.64919269719403	3.20977648001853
C	-0.56354428505111	-2.65266824218738	1.80302524936938
H	0.39449431731543	-3.17650893124556	1.71071302261470
H	-1.32928185763521	-3.18538041602983	1.22776460816763
H	-0.86043406395136	-2.56761055077900	2.85526726488231
C	-3.50073243015834	2.16249383602617	2.15017538376180
H	-4.29513084741719	2.34973321891833	1.41421225810568
H	-3.62714358351304	2.89533823987932	2.96086513322772
H	-3.67343927227518	1.16617120023489	2.58811385967536
C	-3.17523615484156	0.92127607763440	-0.79803537052355
H	-3.02148088422251	0.06472696014470	-1.47300870495983
H	-4.01471974041391	0.67085243872798	-0.12940745668905
C	-2.10632891551601	2.30656623710447	1.53262702029965
H	-1.31892788871722	2.24381744108947	2.29876347608723
H	-1.98334472186361	3.29522610922418	1.06376427550894
C	-3.45937578884104	2.19812687841997	-1.59754906736986
H	-4.37317370694159	2.07155827803626	-2.19553986879605
H	-2.63235841685138	2.42754571413929	-2.28384701395601
H	-3.60729909399943	3.06815251586318	-0.94057698370465
C	-0.07162303861920	-4.76251382376081	-1.62635460534209
Cl	1.06626910349221	-5.12153765385077	-0.29150821709304
N	-0.40982387391310	-1.27129394301093	1.23647870351449
H	-0.08609208189072	-1.33883223717412	0.24121446612213
C	-1.73374876868391	-0.55605648485004	1.17442753380615
H	-2.07489538588568	-0.41385776799179	2.20951425358649
H	-2.43198351171916	-1.22535478326561	0.65403698893435

H	-0.96720373571430	-5.37379385796323	-1.49154287028714
Cl	-0.59125643451668	-3.03014684593261	-1.68064592355100
H	0.43564229057969	-4.96774605405686	-2.57246123842818

References

1. C. J. Curtis, A. Miedaner, R. Ciancanelli, W. W. Ellis, B. C. Noll, M. Rakowski DuBois and D. L. DuBois, *Inorg. Chem.*, 2003, **42**, 216-227.
2. J. M. Darmon, S. Raugei, T. Liu, E. B. Hulley, C. J. Weiss, R. M. Bullock and M. L. Helm, *ACS Catal.*, 2014, **4**, 1246-1260.
3. E. B. Hulley, K. D. Welch, A. M. Appel, D. L. DuBois and R. M. Bullock, *J. Am. Chem. Soc.*, 2013, **135**, 11736-11739.
4. C. J. Weiss, J. D. Egbert, S. Chen, M. L. Helm, R. M. Bullock and M. T. Mock, *Organometallics*, 2014, **33**, 2189-2200.
5. R. B. King and F. G. A. Stone, *Inorg. Synth.*, 1963, **7**, 110-112.
6. S. A. Keppie and M. F. Lappert, *J. Organomet. Chem.*, 1969, **19**, P5-P6.
7. P. Leoni, A. Landi and M. Pasquali, *J. Organomet. Chem.*, 1987, **321**, 365-369.
8. J. Le Bras, H. Jiao, W. E. Meyer, F. Hampel and J. A. Gladysz, *J. Organomet. Chem.*, 2000, **616**, 54-66.
9. P. Jutzi, C. Müller, A. Stammler and H.-G. Stammler, *Organometallics*, 2000, **19**, 1442-1444.
10. R. J. LeSuer, C. Buttolph and W. E. Geiger, *Anal. Chem.*, 2004, **76**, 6395-6401.
11. Bruker *SAINT Program for Data Reduction*, Bruker AXS, Inc., Madison, WI, USA, 2007.
12. Bruker *SADABS Program for Data Reduction*, Bruker AXS Inc., Madison, WI, USA, 2007.
13. O. V. Dolomanov, L. J. Bourhis, R. J. Gildea, J. A. K. Howard and H. Puschmann, *Journal of Applied Crystallography*, 2009, **42**, 339-341.
14. A. D. Becke, *Phys. Rev. A*, 1988, **38**, 3098-3100.
15. J. P. Perdew, *Phys. Rev. B*, 1986, **33**, 8822-8824.
16. C. S. Letko, J. A. Panetier, M. Head-Gordon and T. D. Tilley, *J. Am. Chem. Soc.*, 2014, **136**, 9364-9376.
17. S. Grimme, S. Ehrlich and L. Goerigk, *J. Comp. Chem.*, 2011, **32**, 1456-1465.
18. S. Grimme, *J. Comp. Chem.* , 2006, **27**, 1787-1799.
19. K. S. Thanthiriwatte, E. G. Hohenstein, L. A. Burns and C. D. Sherrill, *J. Chem. Theory Comput.*, 2011, **7**, 88-96.
20. R. Krishnan, J. S. Binkley, R. Seeger and J. A. Pople, *J. Chem. Phys.*, 1980, **72**, 650-654.
21. T. Clark, J. Chandrasekhar, G. W. Spitznagel and P. von Ragué Schleyer, *J. Comput. Chem.*, 1983, **4**, 294-301.
22. J. M. L. Martin and A. Sundermann, *J. Chem. Phys.*, 2001, **114**, 3408-3420.
23. S. Grimme, *Chem. Eur. J.*, 2012, **18**, 9955-9964.
24. A. V. Marenich, C. J. Cramer and D. G. Truhlar, *J. Phys. Chem. B*, 2009, **113**, 6378-6396.
25. F. Neese, *Wiley Interdiscip. Rev.: Comput. Mol. Sci.*, 2017, **8**, e1327.
26. E. D. Glendening, C. R. Landis and F. Weinhold, *J. Comput. Chem.*, 2013, **34**, 1429-1437.
27. W. J. Hehre, R. Ditchfie and J. A. Pople, *J. Chem. Phys.*, 1972, **56**, 2257-2261.
28. M. T. Huynh, W. Wang, T. B. Rauchfuss and S. Hammes-Schiffer, *Inorg. Chem.*, 2014, **53**, 10301-10311.